CONFIGURATION OF SHELL STRUCTURES FOR OPTIMUM STRESSES

by

Howard Paul Harrenstien

A Dissertation Submitted to the
Graduate Faculty in Partial Fulfillment of
The Requirements for the Degree of
DOCTOR OF PHILOSOPHY

Major Subject: Theoretical and Applied Mechanics

Approved:

Signature was redacted for privacy.
In Charge of Major Work

Signature was redacted for privacy.
Head of Major Department

Signature was redacted for privacy.
Dean of Graduate College

Iowa State College
Ames, Iowa
1959

TABLE OF CONTENTS

INTRODUCTION

Shell structures in general are not new concepts. Man observed these structures in nature for countless ages. Some of the more common examples of shells that he found were the eggshell, the shell of a turtle, sea shells of various shapes, the shells of gourds and coconuts, and others too numerous to mention. Apparently he observed that in many of these cases, the natural shells possessed great strength when due consideration was given to their construction material. It is the nature of shell structures to resist applied loads largely by direct stress rather than by bending. It is this item which is largely responsible for their efficient structural behavior.

The first major application of the inherent strength of the shell structure by man (very possibly after an observation of nature) was probably that of the Romans. This first application was in the form of a singly-curved shell structure, i. e., the arch or vault. Later developments produced the doubly-curved arch, or dome, which was in part an outgrowth of the groined vault--a roof structure composed of two intersecting vaults.

There are three important reasons for the development of the arch, vault and dome forms:

1. Churches and other monumental structures required the roofing of large areas.

2. Cut stone was the major building material. For obvious reasons, this cut stone had to be placed so that tensile stresses under working loads would be at a minimum. The arch, vault and dome structures tended to produce compressive stresses in the stone under action of dead and common live loads by virtue of their geometry, and therefore were ideal structural forms as far as cut stone was concerned.
3. Great emphasis was placed on beauty of form and grace of line as well as inclosure of space. These forms by their very nature were considered beautiful and esthetically pleasing.

In present times, the arch and dome form are being revived. In addition to these forms, it may be observed that many new types are being used which have had their birth only in recent years. A few of the more common types of shell structures currently being built are the parabolic arch, spherical or paraboloidal shell, the conoid, and other symmetrical indefinite forms.

The parabolic arch has had its largest application to bridges and aircraft hangers. It was selected for these uses for various reasons. One such reason is that this shape insures uniform compressive stress across a given cross-section when the arch is loaded with a vertical load

uniformly distributed with respect to a horizontal projection. It is in part this stress distribution which enables the arch to span long distances and large areas efficiently. A second reason for its use is the wonderful beauty of form and line it possesses when properly oriented and integrated with its surrounding structure.

The spherical or paraboloidal shell has been used largely in modern-day copies of Renaissance structures and in roofing various large circular areas. The reasons for its use may vary from eclectic practices of architects and clients to the recognition of the inherent efficiency of such a shape when loaded with distributed vertical loads. The relative ease of forming a surface of revolution undoubtedly played a significant role in the selection of this type of shell. As in the case of the parabolic arch, this shape is architecturally pleasing when properly used.

The elliptical shell has applications in the vaulting of areas where boundaries are elliptical. It possesses some of the structural efficiency of the spherical shell, which is merely a special case of an elliptical shell. Formwork is somewhat more difficult in that this shape is not a surface of revolution about a vertical axis.

The hyperbolic paraboloid is probably the most versatile of the present-day shell structures. It had its birth as a structural form only in the past decades. Two of the main reasons for its widespread popularity are that it may be

formed from straight stock because of its straight-line generators and that it possesses a simplicity of stress distribution when it is properly supported and when subjected to a uniformly distributed vertical load. Another reason for its popularity is the large amount of publicity that has recently been given to the structures of Felix Candela, a Mexican architect of rare talent and versatility. The hyperbolic paraboloid is well adapted to the vaulting of a variety of rectangular and skewed areas. When handled by the skilled architect, it possesses a contemporary beauty of form which leaves little to be desired esthetically.

The conoid is surface of revolution which is unlike the spherical or paraboloidal shell in that it is anti-clastic, i. e., its principal curvatures are of opposite sign. It possesses an efficiency of stress distribution when supported and loaded at the edges and center respectively.

The other forms which are in general the non-symmetrical indefinite forms are those forms which are not of any of the previous classes but are invariably doubly-curved. These forms may exhibit favorable or unfavorable stress distribution depending on the methods by which they are selected and loaded. Usually they are conceived to produce some architectural effect rather than for efficiency of structure. It is hoped that this investigation will make possible a design efficiency in these structures heretofore unrealized.

One of the major disadvantages of the previously mentioned shell structures is their inability to exhibit entirely uniform constant stress distribution under an anticipated loading condition. Reasons for calling this a disadvantage vary with the materials used in the shell construction. For shells constructed of materials weak in tension (concrete, stone, plaster, etc.) non-uniform stress distribution may well produce tensile stresses on some plane. These tensile stresses may be resisted by adding reinforcement, increasing the shell thickness, or prestressing to place them back into compression. Each of these remedial measures is to some degree an expression of the inefficiency of the original structure to accept its applied loads.

In the case of materials strong in tension but weak in compression because of their small thickness, non-uniform stress distribution may produce compressive stresses in some plane. These compressive stresses tend to produce buckling. Buckling may be resisted by adding stiffening ribs, supplying more material, or pre-tensioning to place them back into tension. Again, each of these remedial measures may be considered an expression of the inefficiency of the original structure.

It is the purpose of this investigation to develop a method by which the configuration of a shell structure may be determined so that it will resist certain applied normal

pressure loads through constant membrane stress. This structure would then not suffer the effects of non-uniform stress distribution which are found to exist in many of the present types of shell structures. The method will be applied to two examples, and the structural behavior of the resulting shells will be observed under action of the design load. Further study along the lines of design by analysis rather than analysis of design will be proposed.

REVIEW OF LITERATURE

A complete literature review of all published papers and books on membrane and shell structures will not be attempted here. Nash (11) lists over 1450 publications written before 1953 on shells and shell-like structures. Inasmuch as publications in this field have greatly accelerated in recent years, it could well be that the total number of publications on this subject alone is in the neighborhood of 3000-5000 at the present time. Fortunately, the number of these papers which relate directly to the problem at hand is not so large.

One of the first investigators in the field of minimum surfaces formed by membranes was J. Plateau (12), (13), (14) in 1864. In his papers titled "Figures of Equilibrium of a Liquid Mass", Plateau uses the basic relationship between curvature, surface tension, and normal pressure which appears as equation 1.9 in Fig. 1 of this investigation to predict the equilibrium configuration for a membrane subjected to given pressures and boundary conditions when withdrawn from the action of gravity. For various conditions of loads and boundaries, he shows that the minimum surfaces arising are the sphere, the plane, the cylinder, the unduloid, the catenoid, and the nodoid.

In 1874, C. W. Merrifield (8) presented the "Determination of the Form of the Dome of Uniform Stress" in which he

applied the principle of initial stipulation of stress in order to predict the proper form of dome required to resist axial live loads, normal pressures and dead load. He developed for this shape a differential equation which contained a factor which was the desired ratio of circumferential to radial stress. His domes were surfaces of revolution and were subject to the following conditions:

1. That the thrust along a meridian shall equal the thrust along the parallel per unit of area at every point.
2. That the normal thickness shall vary in such a manner that the area under compression shall be proportional to the thrust.

The first of these conditions would seem to eliminate the inclusion of any factor expressing the ratio of principal stresses as found in the developed equation. Merrifield mentions the economy of his method of design as applied to stone construction.

The next apparent consideration of this means of design was by Von G. Borkhausen (2) in 1900. In his article, the translated title of which is "New Forms for Tanks", he considers equalization of stresses in the design of bottom surfaces of water tanks. He uses a free-body-diagram approach along with the principles of statics.

In 1927, Poschl (15) published an article on domes with equal normal stresses. A procedure for finding domes of

revolution which will have constant normal stress at each point is well presented and examples are included. The approach is that of solving the governing equation for curvature which is basically the same as equation 1.9 of Fig. 1.

In 1952, Jenkins (6) presented a paper at the Symposium on Concrete Shell Roof Construction in which he briefly mentioned a finite difference approach and more thoroughly presented a matrix method in curvilinear coordinates which is applicable to the solution of shell problems. This method is fundamentally one of minimizing the potential energy function. By using the matrix method and electronic computers, Jenkins indicates how stresses and deflections may be predicted for a shell of any shape. It is thought that this method has merit for the analysis of the structural behavior of shells of the type which are predicted by the present investigation when such shells are subjected to loads other than the design loads.

In his article, "Shells with Zero Bending Stresses", Horne (5) in 1953 presented a method by which shells of revolution may be determined which will be free from bending stresses when the applied load is any uniform axial force. Consideration is given to shells of varying thickness, but particular attention is paid to shells whose thickness is uniform. The possibilities of providing boundary rings to prevent local bending stresses in the vicinity of the end sections is investigated.

It is interesting to observe that on page 124 of Horne's paper, he presents the solution which gives rise to constant normal stresses. This solution is found to agree with that of example one of the present investigation. It will be observed in the following section on development of theory that the bending stresses are assumed to be equal to zero in this investigation but that this item is not necessarily assured. However, in the case of example one, the theoretical bending stresses are apparently zero, according to Horne.

In 1957, K. Karas (7) presented closed-form solutions to the Poisson equation for various circular and circular-ringed membranes under hydrostatic pressure. This paper is not directly applicable to the investigation presented here but it does present some interesting inverse solutions to equations 1.10 and 1.11 which appear in the following section on development of theory.

To summarize this literature review, it may be observed that previous investigators have presented the approach of the determination of the form of a shell structure by virtue of the initial stipulation of stresses or physical behavior. However, it is felt that there is yet to be developed a general method for the solution of the pertinent characteristic equations which can be easily and economically applied. It is hoped that the following investigation will serve as a step in the direction of the attainment of such a goal.

DEVELOPMENT OF THEORY

The theoretical relationships involved in this investigation are developed in three parts. The first contains the development of the general differential or characteristic equations which describe the surface that a shell structure must adopt in order that it resist normal pressure loads under constant membrane stresses. This development consists of observing the simplifications that are produced in the general equilibrium equations for stresses in shell structures when the requirement of constant stress is imposed upon them. The second part is an investigation of an analog which gives rise to similar characteristic equations. This analog is that of the equilibrium configuration assumed by an ideal membrane when the membrane is subjected to normal pressure loading. The third part contains the application of the principles of similitude (9) to obtain the required design equations and prediction equations which relate the behavior of the model of part two to the prototype condition of part one.

The details of the procedure described above for part one of this development are given in Fig. 1. The notation and boundary conditions used in Fig. 1 follow.

Let ξ_1 and ξ_2 be the curvilinear distances along the parametric curves ξ_1 = constant and ξ_2 = constant which are assumed to be orthogonal lines of curvature. Define α_1

and α_2 such that $(ds)^2 = \alpha_1^2 d\xi_1^2 + \alpha_2^2 d\xi_2^2$ where ds is the differential arc length along the surface. Denote by x and y the directions of the tangents to the curvilinear coordinates at the point. Denote by z the direction of the principal normal at that point. Let R_1 and R_2 be principal radii of curvature at the point. N_1 and N_2 are the resultant normal forces per unit length acting on the yz and xz faces respectively. M_1 and M_2 are resultant normal moments per unit length acting as shown in Fig. 1. N_{12} and N_{21} are shear forces per unit length lying in the plane of the middle surface as shown. Q_1 and Q_2 are shear forces per unit length acting normal to the middle surface. M_{12} and M_{21} are twisting moments per unit length. The components of the pressure load in the x, y, and z directions are p_1, p_2, and p_3 respectively. The sketch in Fig. 1 merely indicates directions of positive quantities. For development of the equilibrium equations cited in Fig. 1, refer to Wang (16).

Conditions used in Fig. 1 in the simplification of the equilibrium equations are that $N_1 = N_2 = S$ (a constant), $M_1 = M_2 = M_{12} = M_{21} = Q_1 = Q_2 = 0$, $N_{12} = N_{21}$ everywhere, $p_1 = p_2 = 0$, $p_3 = -p$, and that $N_{12} = N_{21} = 0$ on the boundary.

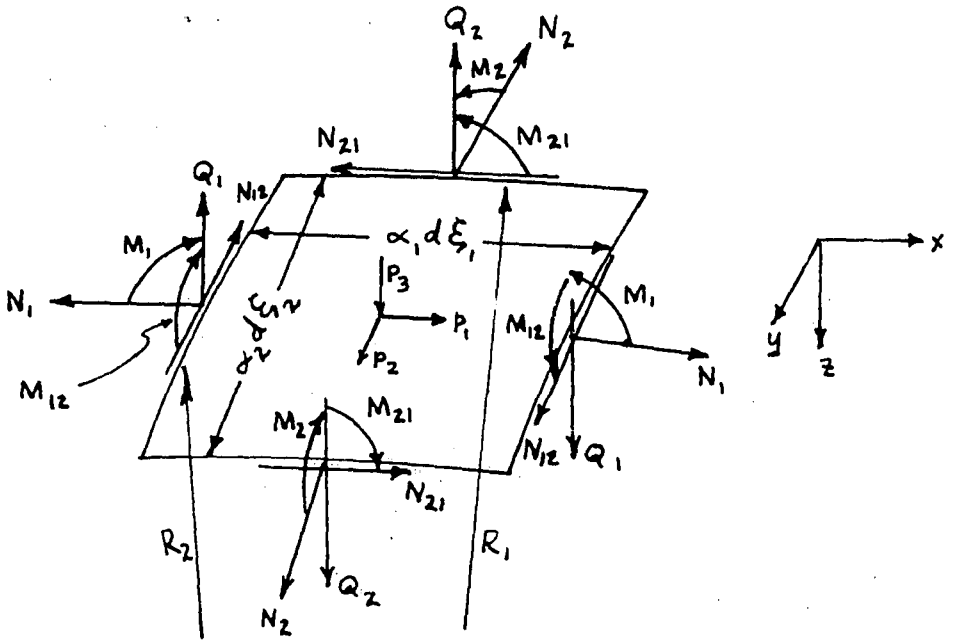

EQUATIONS OF EQUILIBRIUM WRITTEN FOR AN ELEMENT OF SHELL MAY BE FOUND IN WANG (17) AND ARE AS FOLLOWS:

$\Sigma F_x = 0$ yields

$$\frac{\partial(\alpha_2 N_1)}{\partial \xi_1} + \frac{\partial(\alpha_1 N_{21})}{\partial \xi_2} + N_{12}\frac{\partial \alpha_1}{\partial \xi_2} - N_2 \frac{\partial \alpha_2}{\partial \xi_1} - Q_1 \frac{\alpha_1 \alpha_2}{R_1} + \alpha_1 \alpha_2 P_1 = 0. \qquad 1.1$$

$\Sigma F_y = 0$ yields

$$\frac{\partial(\alpha_1 N_2)}{\partial \xi_2} + \frac{\partial(\alpha_2 N_{12})}{\partial \xi_1} + N_{21}\frac{\partial \alpha_2}{\partial \xi_1} - N_1 \frac{\partial \alpha_1}{\partial \xi_2} - Q_2 \frac{\alpha_1 \alpha_2}{R_2} + \alpha_1 \alpha_2 P_2 = 0. \qquad 1.2$$

$\Sigma F_z = 0$ yields

$$\frac{\partial(\alpha_2 Q_1)}{\partial \xi_1} + \frac{\partial(\alpha_2 Q_2)}{\partial \xi_2} + N_1 \frac{\alpha_1 \alpha_2}{R_1} + N_2 \frac{\alpha_1 \alpha_2}{R_2} + \alpha_1 \alpha_2 P_3 = 0. \qquad 1.3$$

Fig. 1. Development of the characteristic equations

$\Sigma M_x = 0$ yields

$$\frac{\partial(\alpha_2 M_{12})}{\partial \xi_1} - \frac{\partial(\alpha_1 M_2)}{\partial \xi_2} + M_1 \frac{\partial \alpha_1}{\partial \xi_2} + M_{21} \frac{\partial \alpha_2}{\partial \xi_1} + Q_2 \alpha_1 \alpha_2 = 0. \quad 1.4$$

$\Sigma M_y = 0$ yields

$$\frac{\partial(\alpha_1 M_{21})}{\partial \xi_2} - \frac{\partial(\alpha_2 M_1)}{\partial \xi_1} + M_2 \frac{\partial \alpha_2}{\partial \xi_1} + M_{12} \frac{\partial \alpha_1}{\partial \xi_2} + Q_1 \alpha_1 \alpha_2 = 0. \quad 1.5$$

DIRECTIONS OF POSITIVE QUANTITIES ARE AS SHOWN ON THE SKETCH.

CONSISTENT WITH THE MEMBRANE THEORY OF SHELLS, ASSUME THAT

$$M_1 = M_2 = M_{21} = M_{12} = Q_1 = Q_2 \equiv 0 .$$

EQUATIONS 1.1 THROUGH 1.5 THEN REDUCE TO

$$\frac{\partial(\alpha_2 N_1)}{\partial \xi_1} + \frac{\partial(\alpha_1 N_{21})}{\partial \xi_2} + N_{12} \frac{\partial \alpha_1}{\partial \xi_2} - N_2 \frac{\partial \alpha_2}{\partial \xi_1} + \alpha_1 \alpha_2 p_1 = 0 , \quad 1.6$$

$$\frac{\partial(\alpha_1 N_2)}{\partial \xi_2} + \frac{\partial(\alpha_2 N_{12})}{\partial \xi_1} + N_{21} \frac{\partial \alpha_2}{\partial \xi_1} - N_1 \frac{\partial \alpha_1}{\partial \xi_2} + \alpha_1 \alpha_2 p_2 = 0 , \quad 1.7$$

and $$N_1 \frac{\alpha_1 \alpha_2}{R_1} + N_2 \frac{\alpha_1 \alpha_2}{R_1} + \alpha_1 \alpha_2 p_3 = 0 . \quad 1.8$$

NOW ASSUME THAT $N_1 = N_2 = S$, $p_1 = p_2 = 0$, $p_3 = -p$ and $N_{12} = N_{21}$,

THEN EQUATION 1.6 BECOMES $\dfrac{\partial(\alpha_1 N_{12})}{\partial \xi_2} + N_{12} \dfrac{\partial \alpha_1}{\partial \xi_2} = 0 .$

This is obviously satisfied by $N_{12} = 0$. If it is assumed that $N_{12} \neq 0$, dividing by $\alpha_1 N_{12}$ gives

$$\frac{1}{\alpha_1 N_{12}} \frac{\partial(\alpha_1 N_{21})}{\partial \xi_2} + \frac{1}{\alpha_1} \frac{\partial \alpha_1}{\partial \xi_2} = 0 .$$

By integration along any curve $\xi_1 = \text{constant}$, it follows that $$\ln(\alpha_1 N_{12}) + \ln \alpha_1 = \ln C_1(\xi_1) .$$

Fig. 1. (continued)

$\therefore \quad N_{12} = \frac{C_1(\xi_1)}{\alpha_1^2}$ along curves ξ_1 = constant .

Since $N_{12} = 0$ at the boundary, $\frac{C_1(\xi_1)}{\alpha_1^2} = 0$ there.

It follows that $C_1(\xi_1) = 0$ and $\therefore N_{12} = 0$ everywhere.

This contradicts the previous assumption that $N_{12} \neq 0$. It then follows that the only value of N_{12} which satisfies equation 1.6 under the conditions assumed is that of zero.

Equation 1.7 becomes $\frac{\partial(\alpha_2 N_{21})}{\partial \xi_1} + N_{21} \frac{\partial \alpha_2}{\partial \xi_1} = 0$,

which is obviously satisfied by $N_{21} = 0$.

If it is assumed that $N_{21} \neq 0$ then by dividing by $\alpha_2 N_{21}$ and by integrating along any curve ξ_2 = constant, it follows that

$$\ln(\alpha_2 N_{21}) + \ln \alpha_2 = \ln C_2(\xi_2) .$$

$\therefore N_{21} = \frac{C_2(\xi_2)}{\alpha_2^2}$ along curves ξ_2 = constant.

From the condition that $N_{21} = 0$ at the boundary, it follows that $C_2(\xi_2) = 0$ and $N_{21} = 0$ which again is a contradiction to the assumption that $N_{21} \neq 0$. It follows that the only value of N_{21} which satisfies equation 1.7 is $N_{21} = 0$.

Thus $N_{12} = N_{21} = 0$ for the conditions specified.

Fig. 1. (continued)

EQUATION 1.8 BECOMES

$$S\left(\frac{\alpha_1 \alpha_2}{R_1}\right) + S\left(\frac{\alpha_1 \alpha_2}{R_1}\right) - \alpha_1 \alpha_2 p = 0$$

$$\text{or} \qquad \frac{1}{R_1} + \frac{1}{R_2} = \frac{p}{S} . \qquad 1.9$$

THIS EQUATION IS THAT RELATIONSHIP WHICH MUST BE SATISFIED BY THE PRINCIPAL CURVATURES OF THE SHELL SURFACE IN ORDER THAT THE ASSUMED CONSTANT STRESS S WILL BE DEVELOPED WHEN THE SHELL IS SUBJECTED TO THE NORMAL PRESSURE p.

IF THE RECIPROCALS OF THE RADII OF CURVATURE ARE APPROXIMATED BY THE SECOND DERIVATIVES OF THE SHELL SURFACE, EQUATION 1.9 BECOMES

$$\frac{\partial^2 z}{\partial x^2} + \frac{\partial^2 z}{\partial y^2} = \frac{p}{S} . \qquad 1.10$$

FOR CASES WHERE $p=0$, EQUATION 1.10 BECOMES

$$\frac{\partial^2 z}{\partial x^2} + \frac{\partial^2 z}{\partial y^2} = 0 . \qquad 1.11$$

IF THE RECIPROCALS OF THE RADII OF CURVATURE ARE REPRESENTED BY THEIR EXACT VALUES, EQUATION 1.9 BECOMES

$$\frac{\frac{\partial^2 z}{\partial x^2}}{\left(1 + \left(\frac{\partial z}{\partial x}\right)^2\right)^{3/2}} + \frac{\frac{\partial^2 z}{\partial y^2}}{\left(1 + \left(\frac{\partial z}{\partial y}\right)^2\right)^{3/2}} = \frac{p}{S} . \qquad 1.12$$

Fig. 1. (continued)

FOR CASES WHERE $p=0$,

$$\frac{\frac{\partial^2 z}{\partial x^2}}{\left(1+\left(\frac{\partial z}{\partial x}\right)^2\right)^{3/2}} + \frac{\frac{\partial^2 z}{\partial y^2}}{\left(1+\left(\frac{\partial z}{\partial y}\right)^2\right)^{3/2}} = 0 \qquad 1.13$$

EQUATIONS 1.10 & 1.11 ARE VALID FOR SHELLS WHOSE SLOPES ARE SMALL. EQUATIONS 1.12 & 1.13 ARE VALID FOR SHELLS WHOSE SLOPES ARE EITHER LARGE OR SMALL.

Fig. 1. (continued)

Equations 1.10 and 1.11 are the characteristic differential equations which describe the surface that a shell structure must adopt in order that it resist normal pressure loads under constant membrane stress. These equations are limited to the case of shells with small surface slopes.

Equations 1.12 and 1.13 are also characteristic equations for the same phenomena but they are not limited in application to shells with small surface slopes as were equations 1.10 and 1.11.

It is obvious that any physical system which has similar characteristic equations may constitute an analog when compared with the original system of part one. One such analog is the behavior of an ideal membrane under normal pressure loads. The development of the characteristic equations for this phenomenon are included in Fig. 2.

CONSIDER A FREE-BODY DIAGRAM OF AN ELEMENT OF AN IDEAL MEMBRANE WHICH IS SUBJECTED TO A NORMAL PRESSURE p:

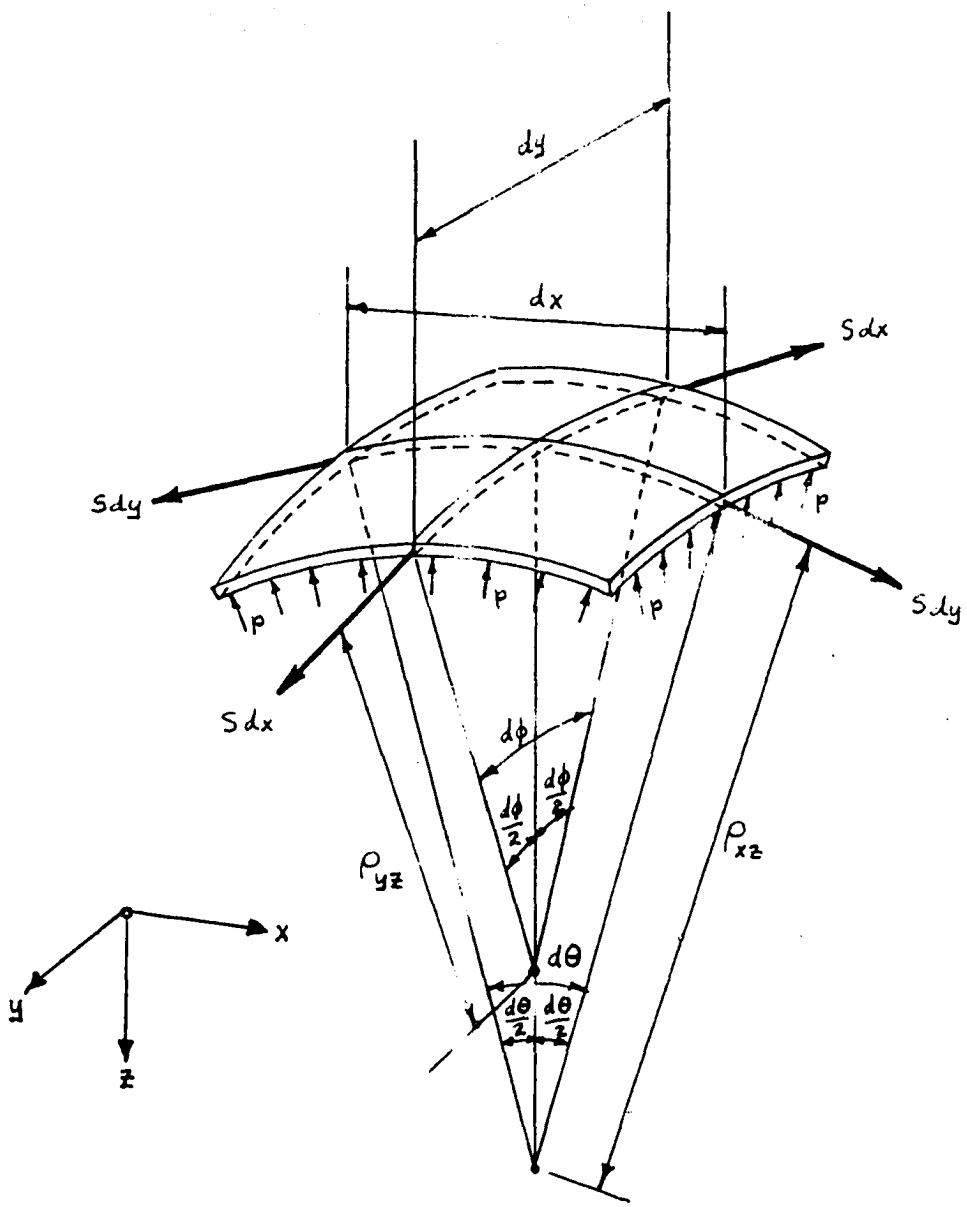

ASSUME THE RESULTANT TENSILE FORCES ON THE CUT SECTIONS ARE TANGENT TO THE TRACES OF THE SURFACE IN THE XZ AND YZ PLANES AS SHOWN.

Fig. 2. Development of the differential equations which govern the deflection of an ideal membrane

$\Sigma F_x = 0$ & $\Sigma F_y = 0$ identically.

$\Sigma F_z = 0$ yields

$$2S\,dy\left(\sin\frac{d\theta}{2}\right) + 2S\,dx\left(\sin\frac{d\phi}{2}\right) = p\,dx\,dy \ ,$$

where p is the pressure,
S is the constant tensile stress,
$d\theta$ is the angle in the XZ-plane,
and $d\phi$ is the angle in the YZ-plane.

Now $\frac{dx}{2} = \rho_{xz}\sin\frac{d\theta}{2}$, from which $\sin\frac{d\theta}{2} = \frac{dx}{\rho_{xz}(2)}$.

Similarly, $\sin\frac{d\phi}{2} = \frac{dy}{\rho_{yz}(2)}$.

Then $2S\,dy\left(\frac{dx}{2\rho_{xz}}\right) + 2S\,dx\left(\frac{dy}{2\rho_{yz}}\right) = p\,dx\,dy$

or $$\frac{1}{\rho_{xz}} + \frac{1}{\rho_{yz}} = \frac{p}{S} \ . \qquad 2.1$$

IF THE RECIPROCALS OF RADII OF CURVATURE ARE APPROXIMATED BY THE SECOND DERIVATIVES AS IN THE PREVIOUS CASE, EQ. 2.1 BECOMES

$$\frac{\partial^2 z}{\partial x^2} + \frac{\partial^2 z}{\partial y^2} = \frac{p}{S} \ , \qquad 2.2$$

WHICH IS A RECOGNIZED FORM OF THE POISSON EQUATION.

FOR CONDITIONS OF ZERO PRESSURE THIS EQ. BECOMES

$$\frac{\partial^2 z}{\partial x^2} + \frac{\partial^2 z}{\partial y^2} = 0 \ , \qquad 2.3$$

WHICH IS RECOGNIZED AS THE LAPLACE EQUATION.

Fig. 2. (continued)

EQUATIONS 2.2 & 2.3 ARE LINEAR DIFFERENTIAL EQUATIONS WHICH GOVERN THE SMALL DISPLACEMENTS OF AN IDEAL MEMBRANE UNDER CONDITIONS OF NORMAL PRESSURE LOADING.

FOR CASES OF LARGE DEFLECTION OR SLOPE THE RECIPROCALS OF THE RADII OF CURVATURE MAY BE EXPRESSED AS

$$\frac{1}{\rho_{xz}} = \frac{\frac{\partial^2 z}{\partial x^2}}{\left(1+\left(\frac{\partial z}{\partial x}\right)^2\right)^{3/2}} \quad \text{and} \quad \frac{1}{\rho_{yz}} = \frac{\frac{\partial^2 z}{\partial y^2}}{\left(1+\left(\frac{\partial z}{\partial y}\right)^2\right)^{3/2}} .$$

EQUATION 2.1 THEN BECOMES

$$\frac{\frac{\partial^2 z}{\partial x^2}}{\left(1+\left(\frac{\partial z}{\partial x}\right)^2\right)^{3/2}} + \frac{\frac{\partial^2 z}{\partial y^2}}{\left(1+\left(\frac{\partial z}{\partial y}\right)^2\right)^{3/2}} = \frac{p}{S} . \quad 2.4$$

FOR CONDITIONS OF ZERO PRESSURE THIS EQUATION BECOMES

$$\frac{\frac{\partial^2 z}{\partial x^2}}{\left(1+\left(\frac{\partial z}{\partial x}\right)^2\right)^{3/2}} + \frac{\frac{\partial^2 z}{\partial y^2}}{\left(1+\left(\frac{\partial z}{\partial y}\right)^2\right)^{3/2}} = 0 . \quad 2.5$$

EQUATIONS 2.4 & 2.5 ARE NON-LINEAR DIFFERENTIAL EQUATIONS GOVERNING THE LARGE DEFLECTIONS OF AN IDEAL MEMBRANE UNDER CONDITIONS OF NORMAL PRESSURE LOADING.

Fig. 2. (continued)

It will be observed that equations 2.2 through 2.5 for the membrane are identical in form to equations 1.10 through 1.13 for the original system. From this observation it is concluded that an analogy exists between the two systems. The required design equations and prediction equations which relate these two systems may be developed through the application of the principles of similitude (9). This development is presented in Fig. 3.

FOR A SHELL STRUCTURE OF THE APPROPRIATE TYPE , ASSUME

$$S = f(p, \ell, \lambda)$$

where S is a membrane stress of dimensions FL^{-1},
p is the normal pressure $\sim FL^{-2}$,
ℓ is a length $\sim L$,
and λ are other lengths $\sim L$.

FOR THE MEMBRANE , ASSUME

$$S_m = f(p_m, \ell_m, \lambda_m).$$

Let $\ell = n_1 \ell_m$ 3.1

and $p = n_2 p_m$ be design conditions 3.2

Now $s = n - b = 4 - 2 = 2\pi$ terms.

Let $\pi_1 = \frac{S}{p\ell}$; $\pi_{1m} = \frac{S_m}{p_m \ell_m}$

$\pi_2 = \frac{\lambda}{\ell}$; $\pi_{2m} = \frac{\lambda_m}{\ell_m}$.

For a true model,

$\pi_1 = \pi_{1m}$, and $\pi_2 = \pi_{2m}$,

$\frac{S}{p\ell} = \frac{S_m}{p_m \ell_m}$, $\frac{\lambda}{\ell} = \frac{\lambda_m}{\ell_m}$,

$\frac{S}{p} = n_1 \frac{S_m}{p_m}$, $\lambda = n_1 \lambda_m$. 3.3

$S = n_1 n_2 S_m$, 3.4

Eq. 3.3 imposes geometrical similarity.

Eq. 3.4 is the prediction equation.

Fig. 3. Similitude relationships

The relationships developed in this section are general and apply to all cases of thin-shell structures which are subjected to normal pressure loads and which satisfy the appropriate equations and boundary conditions. For purposes of illustration and verification of the theory, the method of solution by membrane analogy which has just been described will be applied to two specific examples. The first of these examples pertains to a shell which is circular, while the second pertains to one which is square in plan. The statement of these examples and their solutions may be found in the following section.

APPLICATION OF THEORY TO TWO SPECIFIC EXAMPLES

As previously stated, two examples are presented. Closed-form solutions of the characteristic equations are obtained for the first example. The second example is solved by use of the analogy described in the previous section. In order that this analogy might be verified, it is used to solve the first example and the results are compared with those of the closed-form solution.

For the first example, consider the configuration that a thin-shell structure must assume in order that it resist a single concentrated normal pressure load under constant normal stress. Let it be required that the bounding edge of the shell be circular in plan and that the resultant of the pressure load act through the center of this bounding circle. Example number two is identical to the first one except that the bounding edge of the shell is to be square in plan.

In general, closed-form solutions to the characteristic equations 1.10 through 1.13 are difficult, if not impossible, to obtain for any but the simplest of problems. Series solutions may be found in many cases which give satisfactory convergence as far as usual engineering accuracy is concerned. Numerical methods, recently on the upswing due to digital computer advances, may be used to solve a great variety of problems, provided that proper convergence is obtained. Analogies such as the one described in the

previous section may be used to advantage if they satisfy the proper requirements of similitude in order to make them valid.

Closed-form solutions to equations 1.10 and 1.11 for the first example were found to be easily obtained by direct integration and are included in Fig. 4. This method of approach was facilitated by the symmetry of the problem.

EXAMPLE #1 MAY BE REPRESENTED BY THE SKETCH TO THE RIGHT.

PRESSURE p IS APPLIED OVER THE CENTRAL REGION $0 \leq r \leq a$.

THE SHELL IS SUPPORTED AT THE EDGE $r = b$.

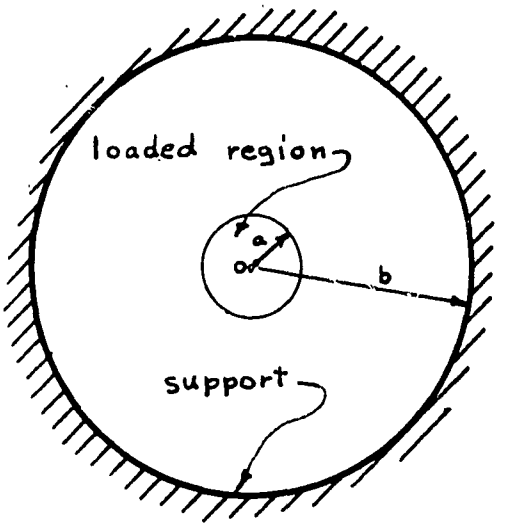

CENTRAL REGION ($0 \leq r \leq a$)

EQ. 1.10 WRITTEN IN TERMS OF CYLINDRICAL COORDINATES INDEPENDENTLY OF Θ BECOMES

$$\frac{d^2z}{dr^2} + \frac{1}{r}\frac{dz}{dr} = \frac{p}{s} \qquad 4.1$$

or $\quad \frac{1}{r}\frac{d}{dr}\left(r\frac{d}{dr}\right)z = \frac{p}{s}$

THEN $\quad \frac{d}{dr}\left(r\frac{d}{dr}\right)z = \frac{pr}{s}$

integrating, $\quad r\frac{dz}{dr} = \frac{pr^2}{2s} + C_1$

$$\frac{dz}{dr} = \frac{pr}{2s} + \frac{C_1}{r}$$

integrating, $\quad z = \frac{pr^2}{4s} + C_1 \ln r + C_2$

When $r=0$, z must be finite $\quad \therefore C_1 = 0$

$$\therefore \quad z = \frac{pr^2}{4s} + C_2 \quad (0 \leq r \leq a) \qquad 4.2$$

$$z\Big|_{r=a} = \frac{pa^2}{4s} + C_2$$

$$\frac{dz}{dr}\Big|_{r=a} = \frac{pa}{2s}$$

Fig. 4. Solutions to equations 1.10 and 1.11 for example one

OUTER REGION ($a \leq r \leq b$)

EQ. 1.11 WRITTEN IN TERMS OF CYLINDRICAL COORDINATES INDEPENDENTLY OF Θ BECOMES

$$\frac{d^2z}{dr^2} + \frac{1}{r}\frac{dz}{dr} = 0 \qquad 4.3$$

or $\frac{1}{r}\frac{d}{dr}\left(r\frac{d}{dz}\right)z = 0$.

Now $z = C_3 \ln r + C_4$ by observation of solution to eqn. 3.1 over central region.

When $r = b$, let $z = 0$

$$0 = C_3 \ln b + C_4$$

$$C_4 = -C_3 \ln b$$

or $z = C_3(\ln r - \ln b) \quad a \leq r \leq b$.

Then $z = C_3 \ln \frac{r}{b}$, 4.4

$$z\Big|_{r=a} = C_3 \ln \frac{a}{b},$$

$$\frac{dz}{dr}\Big|_{r=a} = \frac{C_3}{a} .$$

Equating $\frac{dz}{dr}\Big|_{r=a}$ From both regions

$$\frac{pa}{2s} = \frac{C_3}{a} \text{ or } C_3 = \frac{pa^2}{2s} .$$

Equating $z|_{r=a}$

$$\frac{pa^2}{4s} + C_2 = \frac{pa^2}{2s} \ln \frac{a}{b} \text{ or } C_2 = \frac{pa^2}{4s}\left(2\ln\frac{a}{b} - 1\right)$$

Fig. 4. (continued)

THE FINAL SOLUTION FOR THE CENTRAL REGION MAY BE WRITTEN

$$z = \frac{pr^2}{4s} + \frac{pa^2}{4s}\left(2\ln\frac{a}{b} - 1\right)$$

$$= \frac{p}{4s}\left(r^2 - a^2\right) + \frac{pa^2}{2s}\ln\frac{a}{b} \qquad 4.5$$

AND FOR THE OUTER REGION

$$z = \frac{pr^2}{2s}\ln\frac{r}{b} \qquad 4.6$$

EQUATIONS 4.5 & 4.6 ARE THE SOLUTIONS TO THE LINEAR DIFFERENTIAL EQUATIONS , 1.10 & 1.11 , WRITTEN FOR EXAMPLE NUMBER ONE .

Fig. 4. (continued)

Equations 4.5 and 4.6 constitute the exact solution to the linear differential equations 1.10 and 1.11 written for example one. Equation 4.5 is applicable over the central region and equation 4.6 is valid over the outer region. This solution is only approximate, however, for the problem at hand because of the approximations which were used for the expressions for curvatures in arriving at equations 1.10 and 1.11. Intuitively, a more "exact" solution should arise out of the closed-form solution of the non-linear characteristic equations 1.12 and 1.13 since these equations involve fewer approximations.

The closed-form solution to these non-linear equations written for example one may be obtained by an inverse method; that is, by the method of the assumption of a solution and the corresponding evaluation of appropriate parameters. The details of this solution are given in Fig. 5.

THE SKETCH IS REPEATED FOR PURPOSES OF REFERENCE.

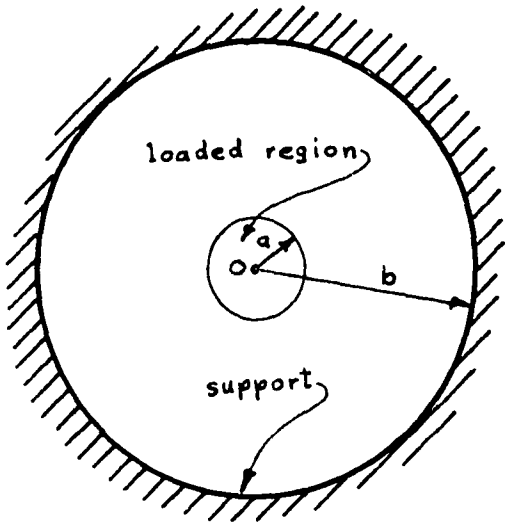

CENTRAL REGION ($0 \leq r \leq a$)

EQ. 1.12 WRITTEN IN TERMS OF CYLINDRICAL COORDINATES INDEPENDENTLY OF Θ BECOMES

$$\frac{1}{r\left(1+\left(\frac{dr}{dz}\right)^2\right)^{1/2}} - \frac{\frac{d^2r}{dz^2}}{\left(1+\left(\frac{dr}{dz}\right)^2\right)^{3/2}} = \frac{p}{S} \cdot \qquad 5.1$$

Assume a solution of the form $r = \sqrt{k^2-(z+c)^2}$,
(It is logical for the surface to be spherical in this case).

Then $\frac{dr}{dz} = -\left(k^2-(z+c)^2\right)^{-1/2}(z+c)$,

and $\frac{d^2r}{dz^2} = -\left(k^2-(z+c)^2\right)^{-1/2}(z+c)^2 - \left(k^2-(z+c)^2\right)^{-1/2}$.

Now $\frac{1}{r\left(1+\left(\frac{dr}{dz}\right)^2\right)^{1/2}} = \frac{1}{\left[k^2-(z+c)^2\right]^{1/2}\left[1+\frac{(z+c)^2}{k^2-(z+c)^2}\right]^{1/2}} = \frac{1}{k}$,

and $\frac{-\frac{d^2r}{dz^2}}{\left(1+\left(\frac{dr}{dz}\right)^2\right)^{3/2}} = \frac{-\left[k^2-(z+c)^2\right]^{-3/2}(z+c)^2 - \left[k^2-(z+c)^2\right]^{-1/2}}{\left[1+\frac{(z+c)^2}{k^2-(z+c)^2}\right]^{3/2}}$

$$= -\frac{-(z+c)^2-k^2+(z+c)^2}{\left[k^2-(z+c)^2+(z+c)^2\right]^{3/2}} = \frac{1}{k} \cdot$$

on substitution $\frac{1}{k} + \frac{1}{k} = \frac{p}{S}$ from which $k = \frac{2S}{p}$.

Fig. 5. Solutions to equations 1.12 and 1.13 for example one

THE SOLUTION FOR THE CENTRAL REGION THEN BECOMES

$$r = \sqrt{\left(\frac{2s}{p}\right)^2 - (z+c)^2}$$

$$\text{or} \quad z = \sqrt{\left(\frac{2s}{p}\right)^2 - r^2} - c \,, \quad (0 \le r \le a) \qquad 5.2$$

OUTER REGION ($a \le r \le b$)

EQ. 1.13 WRITTEN IN TERMS OF CYLINDRICAL COORDINATES INDEPENDENTLY OF Θ BECOMES

$$\frac{1}{r\left(1+\left(\frac{dr}{dz}\right)^2\right)^{1/2}} - \frac{\frac{d^2r}{dz^2}}{\left(1+\left(\frac{dr}{dz}\right)^2\right)^{3/2}} = 0 \qquad 5.3$$

$$\text{or} \quad \frac{1}{r} = \frac{\frac{d^2r}{dz^2}}{1+\left(\frac{dr}{dz}\right)^2} \,,$$

$$\text{From which} \quad r\frac{d^2r}{dz^2} - \left(\frac{dr}{dz}\right)^2 - 1 = 0 \,. \qquad 5.4$$

Assume a solution of the form $z = C_1 - K_1 \cosh^{-1}\left(\frac{r}{K_1}\right)$.

Taking deriv. with respect to z ;

$$1 = -K_1 \left(\frac{1}{\sqrt{\left(\frac{r}{K_1}\right)^2 - 1}}\right)\left(\frac{1}{K_1}\right)\frac{dr}{dz}$$

$$\text{or} \quad \frac{dr}{dz} = -\sqrt{\left(\frac{r}{K_1}\right)^2 - 1} \,.$$

$$\text{Then} \quad \left(\frac{dr}{dz}\right)^2 = \left(\frac{r}{K_1}\right)^2 - 1 \,.$$

$$\text{Now} \quad \frac{d^2r}{dz^2} = \frac{-1}{2}\left(\left(\frac{r}{K_1}\right)^2 - 1\right)^{-1/2}\left(\frac{2r}{K_1^2}\right)\frac{dr}{dz}$$

$$= \left[\left(\frac{r}{K_1}\right)^2 - 1\right]^{-1/2}\left(\frac{r}{K_1^2}\right)\left[\left(\frac{r}{K_1}\right)^2 - 1\right]^{1/2} = \frac{r}{K_1^2} \,,$$

Note: The form of the above assumed solution was found by integrating the differential equation obtained by $\Sigma F_z = 0$ on the free-body diagram in the section on comparison of experimental and theoretical results.

Fig. 5. (continued)

and $r\frac{d^2r}{dz^2} = r\left(\frac{r}{K_1^2}\right) = \frac{r^2}{K_1^2}$.

Also $\left(\frac{dr}{dz}\right)^2 = \frac{r^2}{K_1^2} - 1$, from before .

Subst into eqn. 5.4 and obtain

$$\frac{r^2}{K_1^2} - \left(\frac{r^2}{K_1^2} - 1\right) - 1 = 0 \quad \text{identically .}$$

$\therefore$ the assumed solution is valid .

Now when $r = b$, $z = 0$,

$$\therefore C_1 = K_1 \cosh^{-1}\left(\frac{b}{K_1}\right) .$$

$$z\Big|_{r=a} = K_1 \cosh^{-1}\left(\frac{b}{K_1}\right) - K_1 \cosh^{-1}\left(\frac{a}{K_1}\right)$$

$$\text{and } \frac{dz}{dr}\Big|_{r=a} = \frac{-1}{\sqrt{\left(\frac{a}{K_1}\right)^2 - 1}}$$

} For outer region.

$$z\Big|_{r=a} = \sqrt{\left(\frac{2s}{p}\right)^2 - a^2} - C$$

$$\text{and } \frac{dz}{dr}\Big|_{r=a} = \frac{-1}{\sqrt{\left(\frac{2s}{pa}\right)^2 - 1}}$$

} For inner region.

Equating slopes let $K_1 = \frac{pa^2}{2s}$.

Equating deflection at $r = a$

$$\sqrt{\left(\frac{2s}{p}\right)^2 - a^2} - C = \frac{pa^2}{2s}\left[\cosh^{-1}\left(\frac{2bs}{pa^2}\right) - \cosh^{-1}\left(\frac{2s}{pa}\right)\right] .$$

Then $$C = \frac{-pa^2}{2s}\left[\cosh^{-1}\left(\frac{2bs}{pa^2}\right) - \cosh^{-1}\left(\frac{2s}{pa}\right)\right] + \sqrt{\left(\frac{2s}{p}\right)^2 - a^2} .$$

Fig. 5. (continued)

THEN THE FINAL SOLUTIONS MAY BE WRITTEN

INNER REGION ($0 \leq r \leq a$)

$$z = \sqrt{\left(\frac{2s}{p}\right)^2 - r^2} - \sqrt{\left(\frac{2s}{p}\right)^2 - a^2} + \frac{pa^2}{2s}\left[\cosh^{-1}\left(\frac{2bs}{pa^2}\right) - \cosh^{-1}\left(\frac{2s}{pa}\right)\right] \qquad 5.5$$

OUTER REGION ($a \leq r \leq b$)

$$z = \frac{pa^2}{2s}\left[\cosh^{-1}\left(\frac{2bs}{pa^2}\right) - \cosh^{-1}\left(\frac{2rs}{pa^2}\right)\right]. \qquad 5.6$$

THESE ARE THE SOLUTIONS TO THE NON-LINEAR DIFFERENTIAL EQUATIONS 1.12 & 1.13 WRITTEN FOR EXAMPLE ONE.

Fig. 5. (continued)

Equations 5.5 and 5.6 constitute the exact solution to the non-linear characteristic equations 1.12 and 1.13 written for example one. Equation 5.5 is applicable over the inner region and equation 5.6 is valid for the outer region.

Closed-form solutions to equations 1.10 through 1.13 for example number two were considered extremely difficult to obtain. Certainly, for the general case of unsymmetrical loading and boundary conditions which would be involved in numerous practical problems, such closed-form solutions would be all but impossible. It was therefore decided that the analogy method should be investigated for the solution to this example. The analogy to be used was that of the ideal membrane, governing equations for which were developed in Fig. 2 and which appeared as equations 2.2 through 2.5. These equations were seen to be identical to equations 1.10 through 1.13. In order that the integrity of this analogy might be verified, it was used to solve example one as well as number two, and the results of the first example were compared with those of the closed-form solution found in equations 5.5 and 5.6. This comparison of results will be reported later in Fig. 8.

The analogy used was economical at the experimental level and it enabled a visual concept of the resulting solution to be obtained immediately. Fig. 6 shows photographs of the apparatus used for constructing, loading and measuring the membranes for the two examples.

Fig. 6. Membrane apparatus

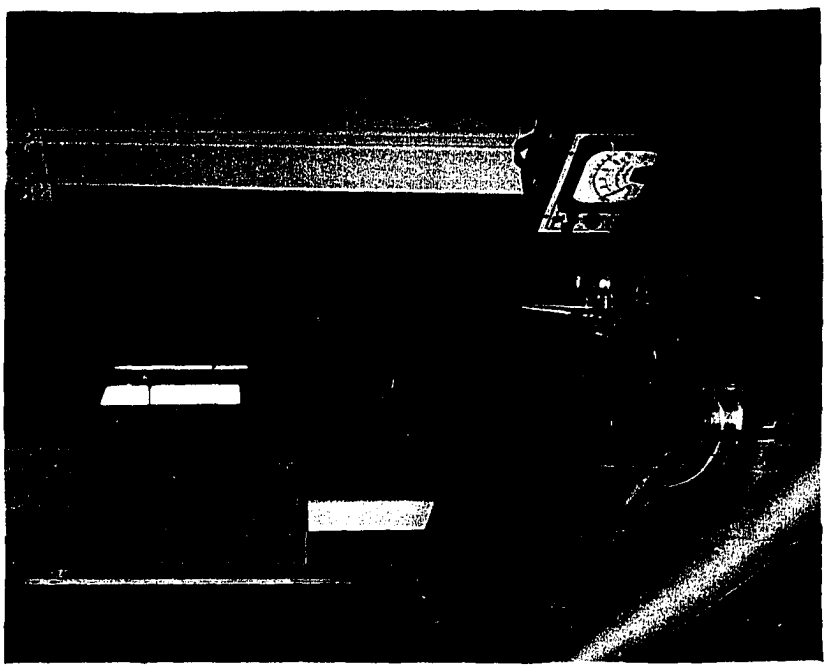

The membrane used was a soap film and the loads were thin aluminum disks of diameter 0.64 in. and weight 0.211 gm. The apparatus was similar in operation to the familiar membrane-analogy machine which is used for predicting torsional stresses and angles of rotation in shafts of constant cross section. The lower photograph shows the apparatus before the membrane was constructed, while the upper photograph shows the membrane for example two in place and being measured. A micrometer needle probe which was attached to a sliding glass cover-plate was used for measuring displacements. The needle was lowered until it contacted the deflected soap film. The instant of contact was determined by measuring the change in resistance between the micrometer needle and the aluminum chassis. Fortunately, the soap film was a reasonably good conductor. When contact was made, the rotating arm on which a sheet of graph paper had been attached was lowered and a needle on top of the micrometer pierced the paper. The micrometer reading gave the elevation of the bubble at the pierced point. It was found that relatively long bubble life was obtained if the experiments were carried out in a humidified atmosphere. In one case, a bubble constructed on Monday morning was still intact on Saturday of the same week. No special soap solution was used, merely a solution of a well-known liquid detergent and water.

Contours of the circular membrane under the load of 0.211 gm. are shown in Fig. 7.

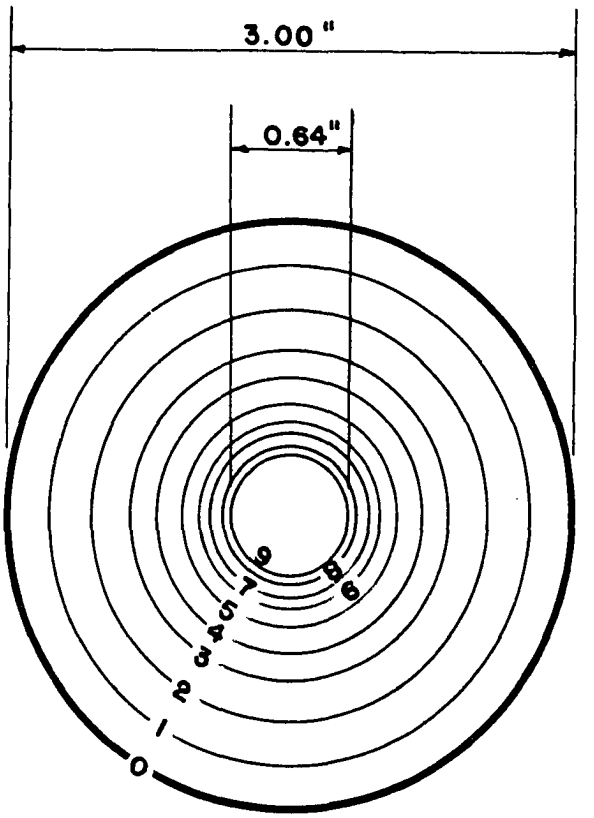

CONTOUR NO.	ELEV. (IN.)
0	0.000
1	0.050
2	0.100
3	0.150
4	0.200
5	0.250
6	0.300
7	0.350
8	0.400
9	0.445

Fig. 7. Contours of membrane for example one

Fig. 8 compares experimentally observed deflections with mathematically determined ones for a radial section.

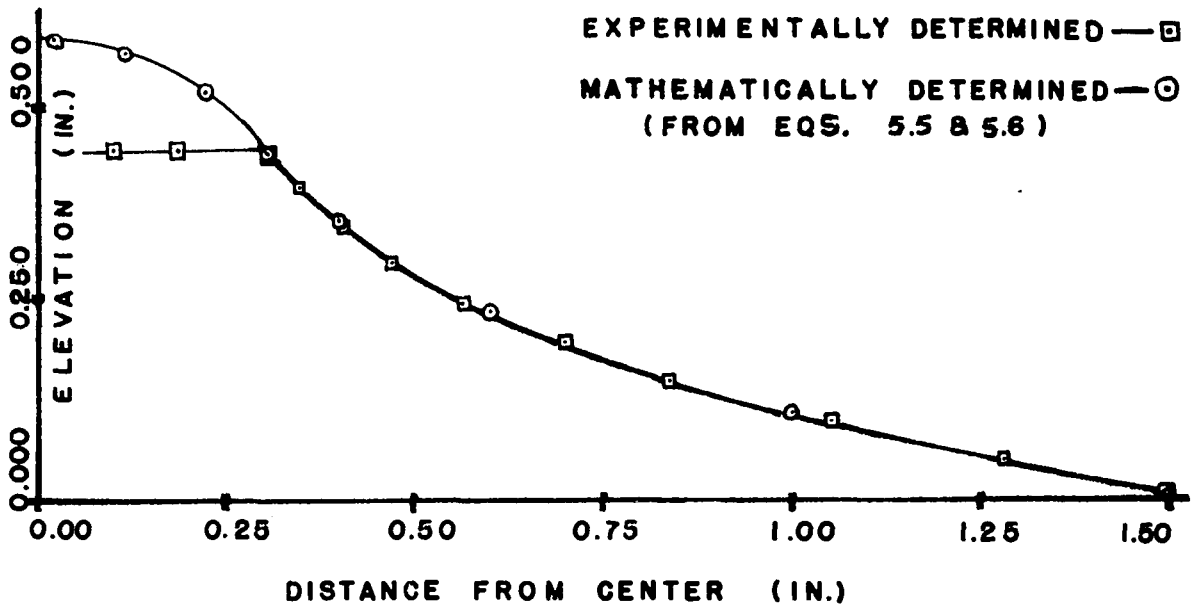

Fig. 8. Graph of radial section for solutions to example one

Because of the apparent closeness of the solutions, it was felt that the membrane solution for the square shell of example two would be valid. The contours for this membrane are shown in Fig. 9.

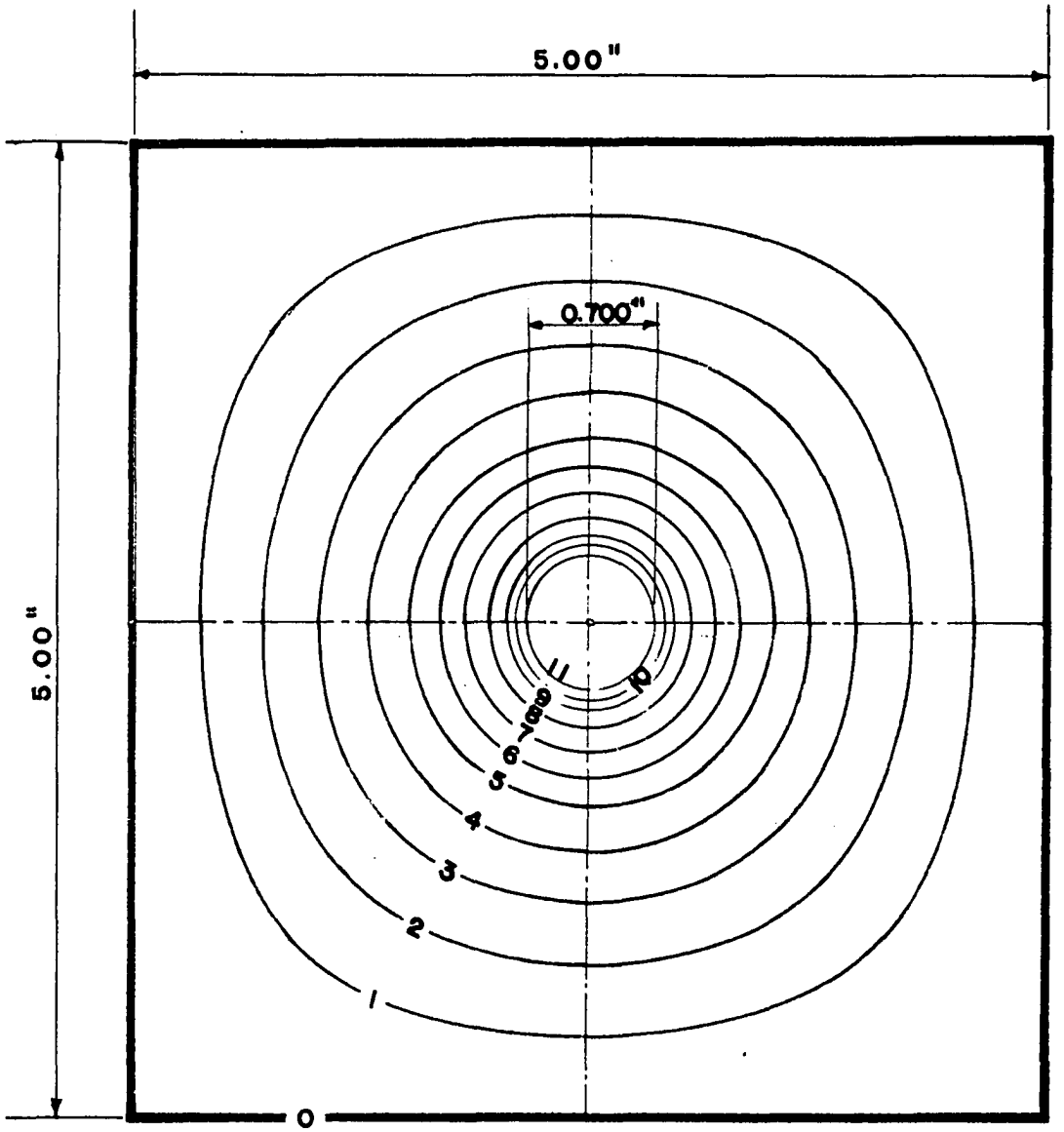

CONTOUR NO.	ELEV. (IN.)	CONTOUR NO.	ELEV. (IN.)
0	0.000	6	0.300
1	0.050	7	0.350
2	0.100	8	0.400
3	0.150	9	0.450
4	0.200	10	0.500
5	0.250	11	0.550

Fig. 9. Contours of membrane for example two

TESTS PERFORMED ON SHELL STRUCTURES CORRESPONDING TO THE TWO SOLUTIONS

Plaster-of-paris shell structures were constructed to conform to dimensions predicted in the previous section for examples one and two. The first shells were approximately 0.25 in. thick and were built to a length scale of 2.5. Molds for these shells were made by applying clay to plywood contours and by making plaster casts of these clay and plywood models. The female mold was made first and the male was merely a direct cast to the female surface. Thus, when the molds were separated $\frac{1}{4}$ in., non-uniform thickness resulted because the top and bottom surfaces had the same curvatures. This method of forming also produced a shell whose central surface had curvatures which were different than those of its outer surfaces and thus were not the desired curvatures. These inaccuracies were thought to be negligible but the stress distribution which was later observed in tests on the resulting shells gave reason to believe that these items could not be neglected. Another factor which undoubtedly affected the stress distribution was that of crudeness of dimensions promoted in part by the small length scale which was used. The upper photograph of Fig. 10 shows the molds that were used for these first shells.

Fig. 10. Molds for plaster-of-paris shells

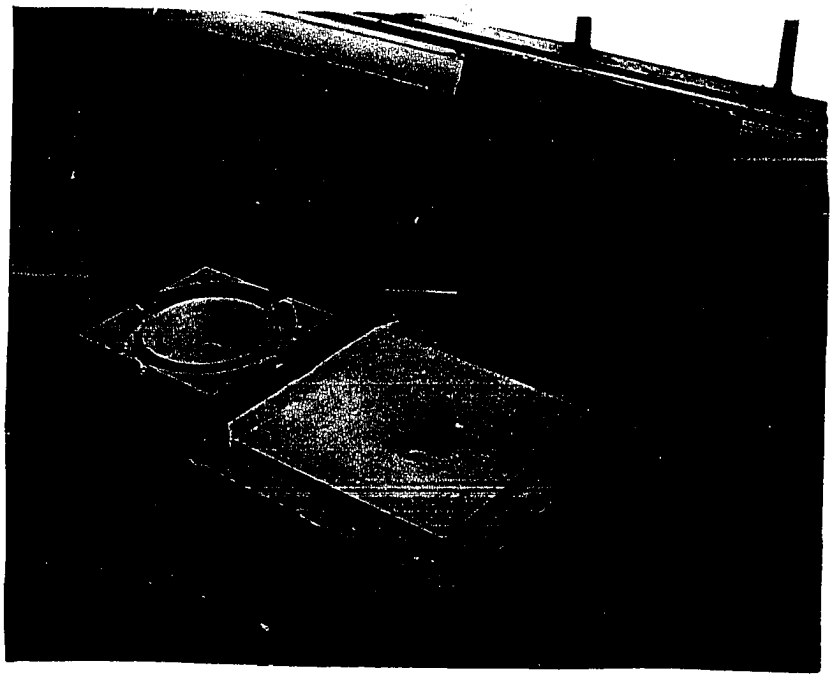

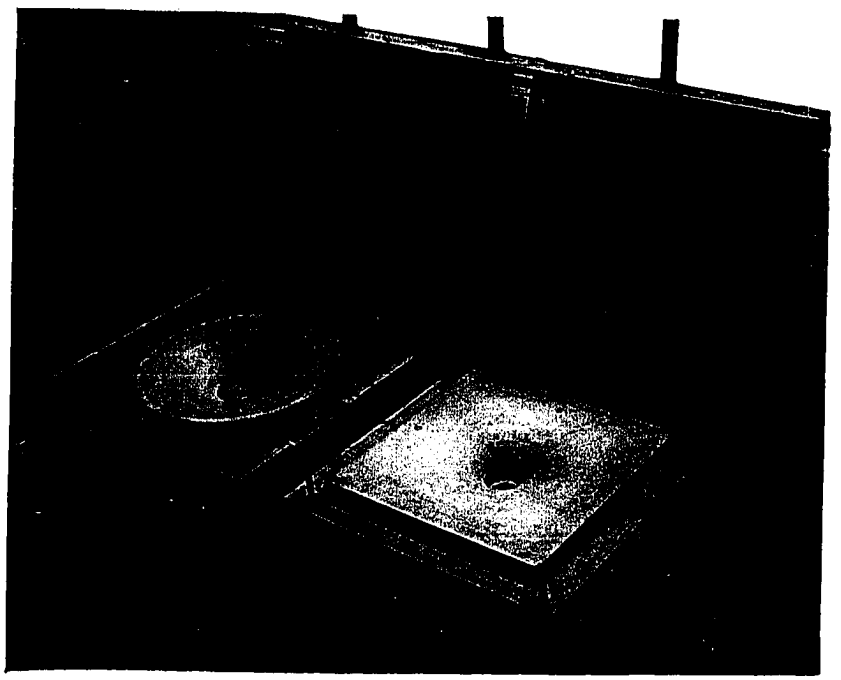

An attempt to produce symmetry of stress distribution resulted in the construction of molds which were built to closer tolerances than the preceding ones. The length scale for the circular shell was increased to 4 while the scale for the square one was held at 2.5 because of dimensional limitations of the testing machine. A scraping technique was employed to bring the clay to dimension by rotating a cutting template about a ½-in. steel shaft as may be seen in Fig. 11. This technique worked extremely well for the circular form and was adapted to the square form by using different templates over different portions of the shell. Separate clay models were made for each surface, thus assuring uniform thickness throughout the resulting shells. Maximum thickness variation in the circular shell was 0.003 in. out of 0.120 in. In the square shell, the thickness was found to vary 0.012 in. out of 0.115 in. Molds for these shells may be seen in the lower photograph of Fig. 10. Photographs of the resulting shells may be seen in Fig. 12.

SR-4 resistance-type strain gages were employed to measure strains from which stresses could be predicted. In order that bending as well as membrane strains could be observed, these gages were placed directly over one another in the positions noted in Fig. 13. All later gage notation refers to this figure. In addition to the strain gages, dial gages were placed as shown in Fig. 12 to measure deflections of the center point with respect to the edges.

Fig. 11. Rotating template apparatus

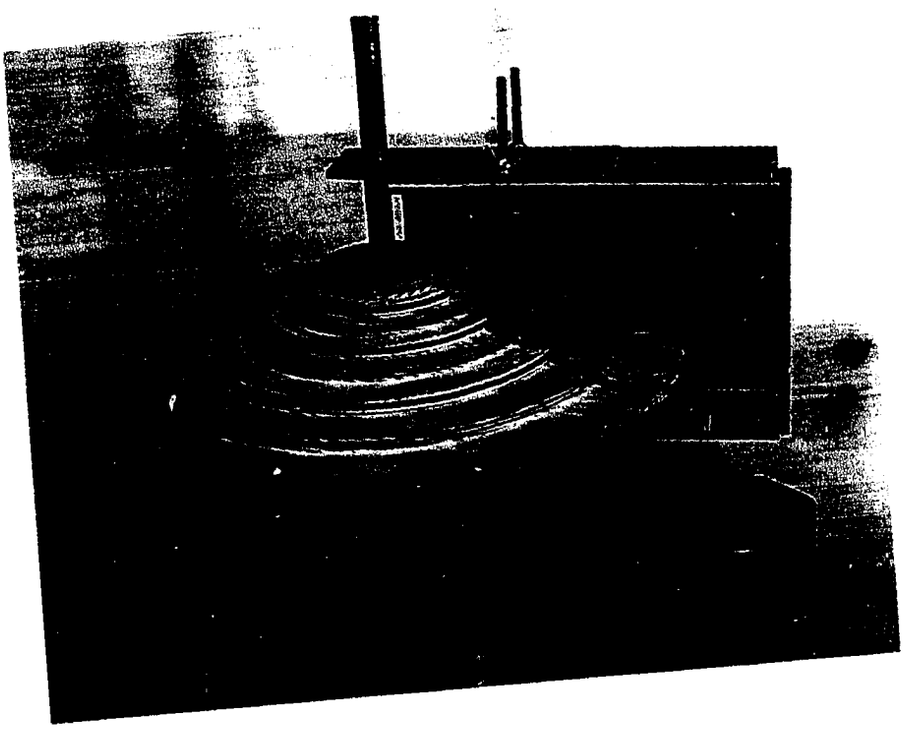

Fig. 12. Plaster-of-paris shells

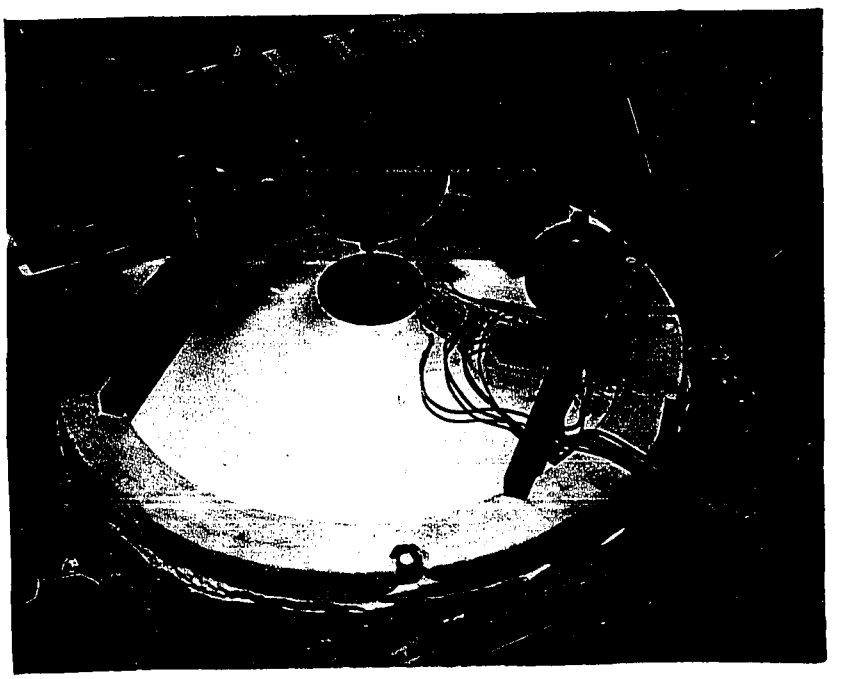

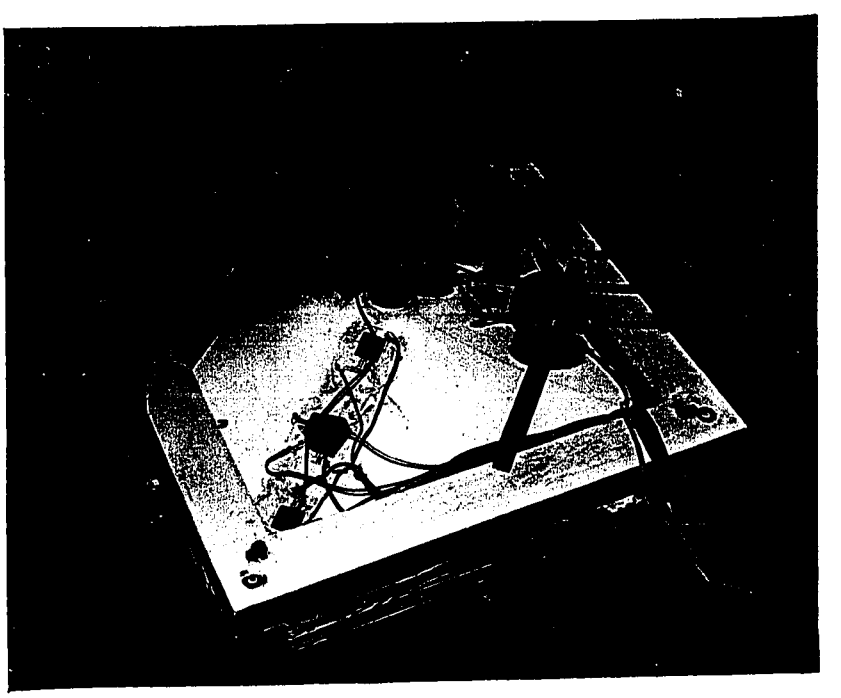

NOTATION : 3tb MEANS GAGE 3t ON THE BOTTOM SURFACE .
3tt MEANS GAGE 3t ON THE TOP SURFACE, ETC.

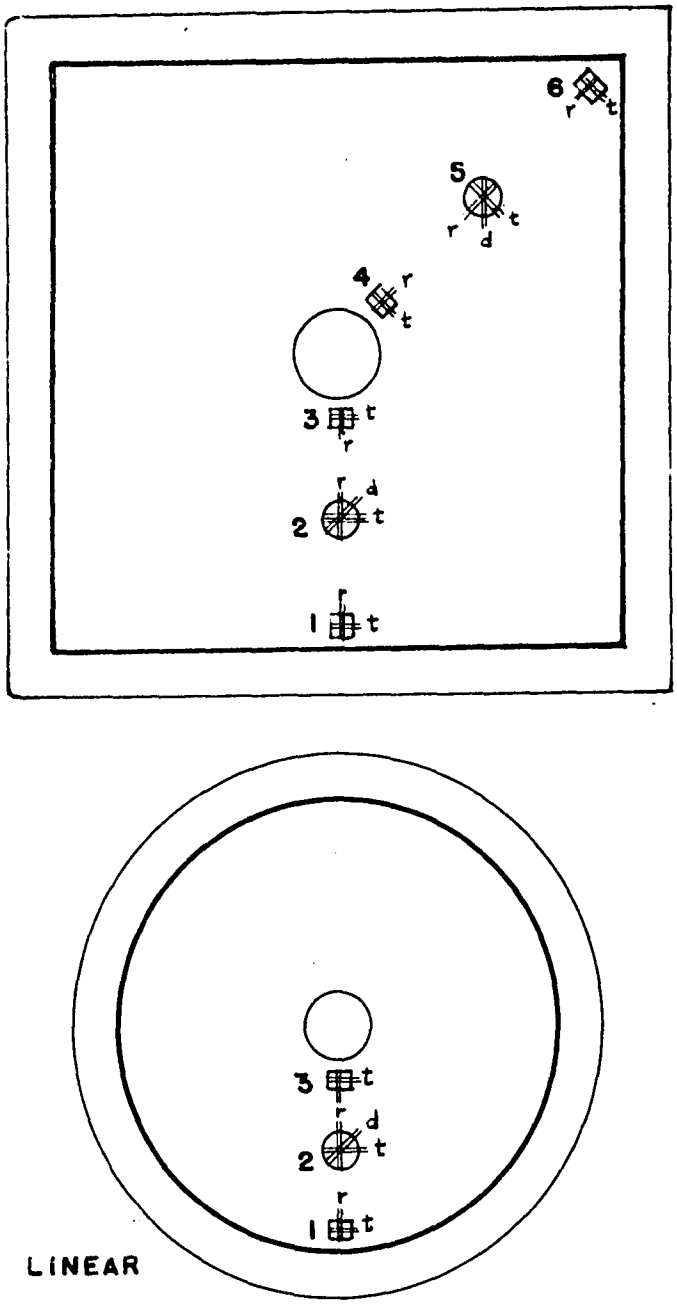

Fig. 13. Location of SR-4 gages

The testing procedure was divided into two stages for each shell. The first stage consisted of measuring only the strains under action of a centered concentrated load which was increased in regular increments from 0 to a load of approximately 150 lb. Fig. 14 shows the square shell in place and being tested. The testing machine was a Tinius-Olsen 20,000 lb hand-crank mechanical type. A "2000 lb" rider was used which allowed a least count of $\frac{1}{2}$ lb. The lower photograph of Fig. 15 shows a closer view of the square shell and the upper photograph shows the circular shell. The large rubber stopper provided a means for uniform transfer of the load to the shells. The second stage of testing consisted of removing the rubber stopper and measuring deflections by the setup of Fig. 12.

In order to observe the effects of various degrees of fixation of edge beams and of various methods of load-transfer at the center point, five load-strain tests were run on the circular shell, each of which involved different edge support and loading methods. In test number one, the shell was placed on the flat aluminum plate; the edge beam was unrestrained. Load transfer at the center was through a rubber stopper. Test number two was conducted the same as the first test except that more gages were used to observe strains at more points in the shell. Test number three consisted of clamping the edge beam rigidly to the aluminum plate. The rubber stopper was used at the center. In the

Fig. 14. View of testing operation

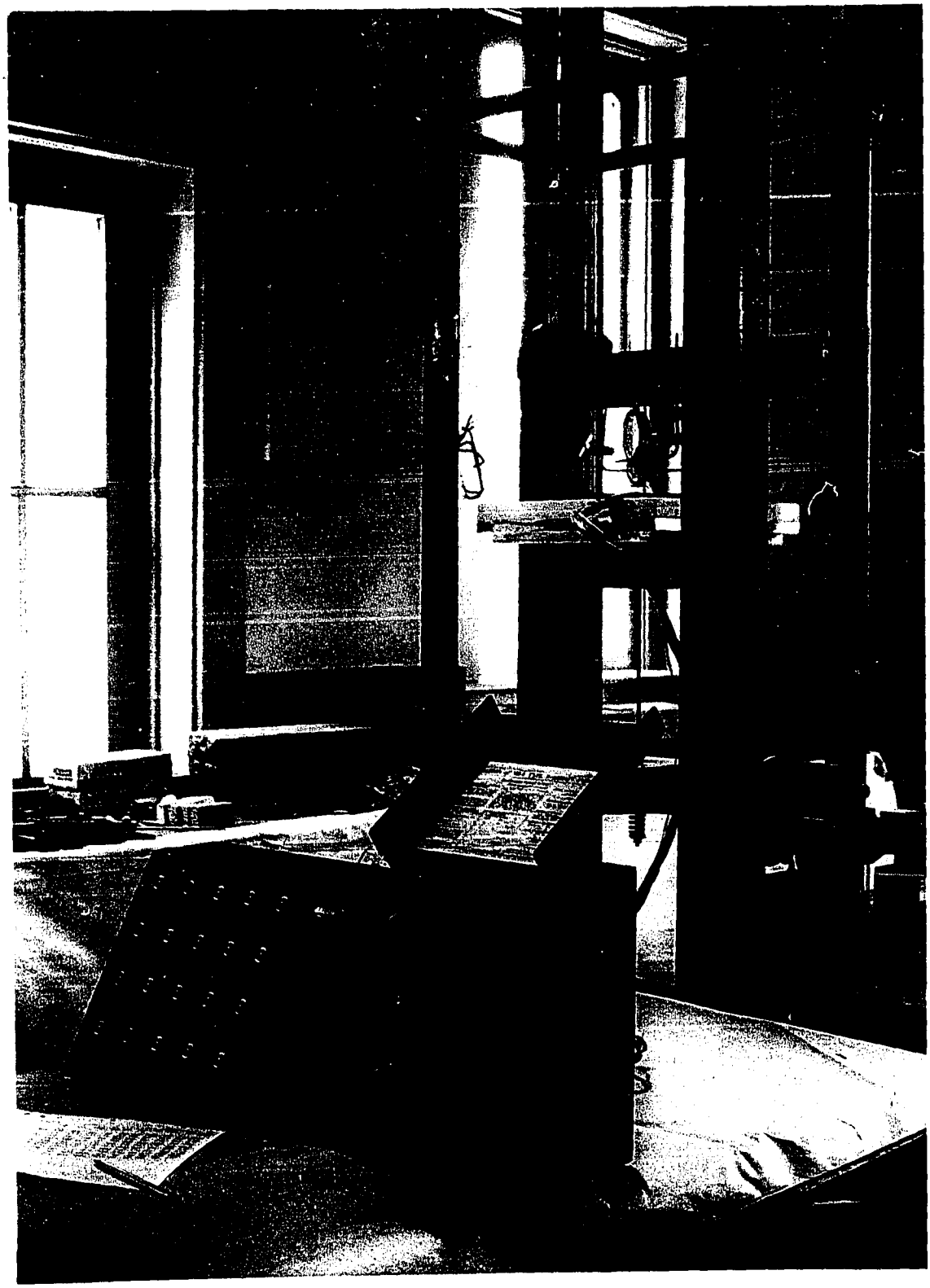

Fig. 15. View of strain test

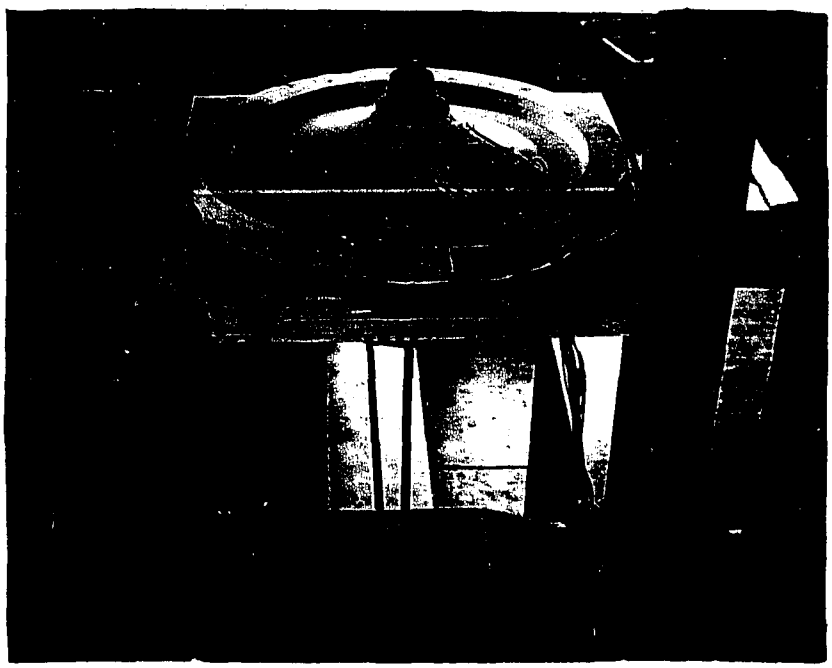

fourth test, the edge beam was both clamped and grouted to the aluminum plate. The rubber stopper was removed from the center and positive bearing by a steel washer was provided. In test number five, the clamps were removed from the edge beam; however, it remained grouted. The rubber stopper was again used.

Load-strain curves were approximately linear throughout the loading range for each of the five tests. The resulting values of the slopes of these curves are listed in Table 1.

Table 1. Slopes[a] of load-strain curves for various tests on circular shell

Point[b]	Test 1	Test 2	Test 3	Test 4	Test 5
1tt	--	0.00	0.00	0.00	0.00
1tb	--	-0.36	-0.22	-0.22	-0.27
1rt	--	0.00	-0.15	-0.15	-0.22
1rb	--	2.22	2.44	2.60	2.22
2tt	1.00	1.16	1.27	1.27	1.14
2tb	1.14	1.20	1.13	1.10	1.06
2rt	1.06	1.39	1.57	1.61	1.42
2rb	0.75	0.72	0.62	0.62	0.51
2dt	1.08	1.42	1.53	1.55	1.32
2db	0.95	1.06	0.70	0.92	0.80
3tt	--	0.35	0.28	0.48	0.20
3tb	--	1.10	0.90	1.10	0.95
3rt	--	0.93	0.87	1.00	0.90
3rb	--	1.10	1.40	1.44	1.07

[a]All slopes are in units of μin. per in. per lb of load. Compressive slopes are positive; tensile slopes are negative.

[b]Notation is as described in Fig. 13.

It will be observed that the various degrees of edge fixation and load application had little effect on these resulting slopes. In further comparisons, the results of test number 4 will be used exclusively.

Slopes of load-strain curves for the square shell are included in Table 2.

Table 2. Slopes[a] of load-strain curves for square shell

Point[b]	Test 1	Point	Test 1
1tt	-0.15	4tt	1.94
1tb	-0.55	4tb	2.37
1rt	0.60	4rt	3.10
1rb	4.15	4rb	1.48
2tt	1.27	5tt	0.92
2tb	1.75	5tb	0.70
2rt	3.95	5rt	1.40
2rb	0.37	5rb	1.37
2dt	3.03	5dt	0.95
2db	0.10	5db	1.30
3tt	2.07	6tt	0.00
3tb	0.64	6tb	-0.56
3rt	1.18	6rt	-0.22
3rb	1.64	6rb	1.35

[a]All slopes are in units of μin. per in. per lb of load. Compressive slopes are positive; tensile slopes are negative.

[b]Notation is as described in Fig. 13.

COMPARISON OF EXPERIMENTAL AND THEORETICAL RESULTS

It is convenient to compare experimental and theoretical results for each shell separately. The first results to be compared will be those for the circular shell, or example one.

The theoretical value of the quantity $S/\bar{P}$ for the circular shell, where P is the resultant vertical component of the pressure load in lb and S is the normal stress in lb per in., was determined from equation 5.6 using the dimensions of the soap-film membrane of Fig. 7. This quantity was then multiplied by the factor representing the effect of the length scale as found by equation 3.4 in order to obtain a predicted value for the normal stress in lb per in. per lb of load. The predicted value for the slope of the load-deflection curve for the center point was determined directly by the application of the principles of strain energy, assuming uniform stress distribution. The details of the procedures described here are included in Fig. 16.

FOR THE PREDICTION OF THE THEORETICAL VALUE OF S/P FOR THE CIRCULAR SHELL, CONSIDER THE FOLLOWING:

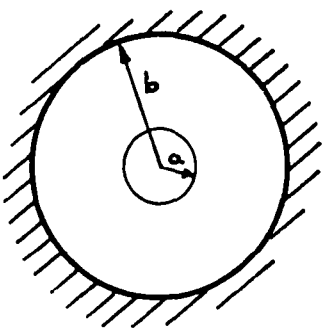

EQ. 5.6 READS

$$z = \frac{pa^2}{2S}\left[\cosh^{-1}\left(\frac{2bS}{pa^2}\right) - \cosh^{-1}\left(\frac{2rS}{pa^2}\right)\right] \qquad a \le r \le b$$

when $r = a$

$$z\Big|_{r=a} = \frac{pa^2}{2S}\left[\cosh^{-1}\left(\frac{2bS}{pa^2}\right) - \cosh^{-1}\left(\frac{2S}{pa}\right)\right]$$

but $p\pi a^2 = P$ or $pa^2 = \frac{P}{\pi}$

Then $$z\Big|_{r=a} = \frac{P}{2\pi S}\left[\cosh^{-1}\left(\frac{2\pi bS}{P}\right) - \cosh^{-1}\left(\frac{2\pi aS}{P}\right)\right].$$

FROM MEASUREMENTS OF SOAP BUBBLE (SEE FIG. 7),

$$z\Big|_{r=a=0.32\,\text{in.}} = 0.445 \text{ in.},$$

$$b = 1.50 \text{ in.}$$

Then $$2\pi(.445)\left(\frac{S_m}{P_m}\right) = \cosh^{-1} 2\pi(1.50)\left(\frac{S_m}{P_m}\right) - \cosh^{-1} 2\pi(.32)\left(\frac{S_m}{P_m}\right).$$

To find the solution to this transcendental eqn., consider the following graph:

Fig. 16. Theoretical values for circular shell

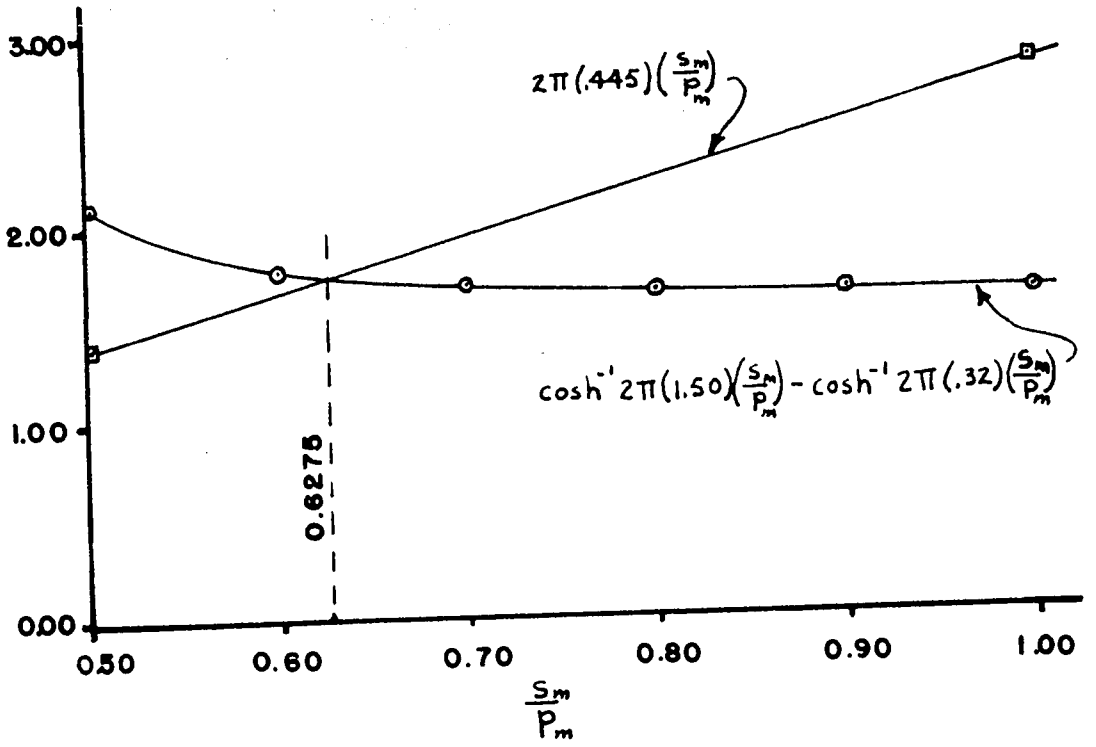

$\frac{S_m}{P_m} = 0.6275$ is the approx. solution to this eqn.

Now $\frac{S}{P} = n_1 \frac{S_m}{P_m}$ from eq. 3.4 .

Let $P = p\pi a^2$ and $P_m = p_m \pi a_m^2$.

Subst. into eq. 3.4 ,

$$\frac{\pi a^2 S}{P} = n_1 \frac{\pi a_m^2 S_m}{P_m} ,$$

$$\frac{S}{P} = n_1 \left(\frac{a_m}{a}\right)^2 \frac{S_m}{P_m} = \frac{1}{n_1} \frac{S_m}{P_m} , \qquad 16.1$$

$\frac{S}{P} = \frac{1}{4}(.6275) = 0.1569$ for circular shell.

Fig. 16. (continued)

FOR THE PREDICTION OF THE SLOPE OF THE LOAD-DEFLECTION CURVE FOR THE CENTERPOINT OF THE CIRCULAR SHELL, CONSIDER THE FOLLOWING:

From Timoshenko and Goodier (16),

$$V = \iiint V_o \, dx\, dy\, dz$$

$$= \iiint \left[\frac{1}{2E}(\sigma_x^2 + \sigma_y^2) - \frac{\mu}{E}\sigma_x\sigma_y + \frac{1}{2G}\gamma_{xy}^2 \right] dx\, dy\, dz .$$

Let $\sigma_x = \sigma_y =$ a constant σ and $\gamma_{xy} = 0$.

Then $$V = \iiint \left(\frac{\sigma^2}{E} - \mu \frac{\sigma^2}{E} \right) dx\, dy\, dz$$

$$= \frac{\sigma^2(1-\mu)}{E} \iiint dx\, dy\, dz . \qquad 16.2$$

Now $$\iiint dx\, dy\, dz = \text{volume} = 2\pi t \int r\, ds$$

$$= 2\pi t \int_{r=a}^{r=b} r \sqrt{1 + \left(\frac{dz}{dr}\right)^2}\, dr \quad \text{for circular shell.}$$

$$\frac{dz}{dr} = -\left[\left(\frac{2sr}{pa^2}\right)^2 - 1 \right]^{-1/2} \qquad a \le r \le b \quad \text{from Fig. 5.}$$

Then $$\text{volume} = 2\pi t \left(\frac{pa^2}{2s}\right)^2 \left[\frac{sr}{pa^2}\sqrt{\left(\frac{2sr}{pa^2}\right)^2 - 1} + \frac{1}{2}\ln \frac{2sr}{pa^2} + \sqrt{\left(\frac{2sr}{pa^2}\right)^2 - 1} \right]_a^b$$

For circular shell $a = 1.28$ in., $b = 6.00$ in., $t = 0.120$ in.,

$$\frac{s}{p} = 0.1569 = \frac{s}{\pi p a^2} .$$

$\therefore$ volume $= 13.8$ in^3.

From eq. 16.2, $V = 13.8\, \sigma^2 \left(\frac{1-\mu}{E} \right)$.

Fig. 16. (continued)

Now $\sigma = \frac{S}{t}$,

$$\therefore V = 13.8 \; S^2 \left(\frac{1-\mu}{t^2 E} \right).$$

$$V_{\text{for 1 lb load}} = 13.8 \left(\frac{S}{P} \right)^2 \left(\frac{1-\mu}{t^2 E} \right) \qquad 16.3$$

$$= 13.8 (.1569)^2 \left[\frac{1 - 0.195}{(.120)^2 (.793 \times 10^6)} \right]$$

$$= 24.4 \times 10^{-6} \text{ in-lb per lb}.$$

(Note that $\mu = 0.195$ and $E = 0.793 \times 10^6$ psi for the circular shell).

The theoretical slope of the load-deflection curve may be found from the above value by considering the area under the load-deflection diagram:

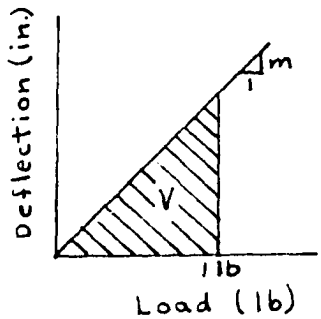

$$V_{\text{for 1 lb load}} = \text{Area} = \tfrac{1}{2}(m)(1) = \frac{m}{2}$$

or $\frac{m}{2} = V$. 16.4

$$\frac{m}{2} = 24.4 \times 10^{-6}$$

and $m = 48.8 \times 10^{-6}$ in./lb.

$$m_{\text{observed}} = 48.0 \times 10^{-6} \text{ in./lb}.$$

Fig. 16. (continued)

From Fig. 16 it is observed that the predicted value of S/P for the circular shell is 0.1569 lb per in. per lb. To compare observed values of S/P and the theoretical value of 0.1569 lb per in. per lb it is possible to convert the observed values of slopes of load-strain curves that are listed in Table 1 to values of S/P at the points where these slopes were observed. This conversion involves the use of the relationship

$$\frac{S_x}{P} = \frac{Et}{(1-\mu^2)}\left(\frac{\epsilon_x}{P} + \mu\frac{\epsilon_y}{P}\right)$$

where S_x is stress in lb per in. in x direction

P is load in lb

E is modulus of elasticity

t is thickness of shell

μ is Poisson's ratio

ϵ_x is unit strain in x direction

ϵ_y is unit strain in y direction

For the circular shell, $E = 0.793 \times 10^6$ psi and $\mu = 0.195$ but t varies from 0.119 in. to 0.122 in. The resulting values of S/P for the circular shell are listed in Table 3.

Table 3. Comparison of values of S/P[a] for gage points on circular shell

Point[b]	Observed S/P	Theoretical S/P	Point	Observed S/P	Theoretical S/P
1tt	-0.003	0.157	2dt	0.177	0.157
1tb	0.029	0.157	2db	0.105	0.157
Avg.[c]	0.013	0.157	Avg.	0.141	0.157
1rt	-0.015	0.157	3tt	0.067	0.157
1rb	0.256	0.157	3tb	0.138	0.157
Avg.	0.120	0.157	Avg.	0.103	0.157
2tt	0.155	0.157	3rt	0.109	0.157
2tb	0.120	0.157	3rb	0.280	0.157
Avg.	0.138	0.157	Avg.	0.194	0.157
2rt	0.182	0.157			
2rb	0.082	0.157			
Avg.	0.132	0.157			

[a]Values of S/P are in units of lb per in. per lb of load. Compressive values are positive; tensile values are negative.

[b]Notation is as described in Fig. 13.

[c]Average values represent membrane stresses.

It will be observed that the average values are the probable membrane stresses which exist at the various points. These averages for the radial gages at points 1, 2 and 3 are 0.120, 0.138 and 0.194 lb per in. per lb, respectively. If it is assumed that the shell is of the exact dimensions predicted by the theory and if it is assumed that the above averages are those stresses which are the resultant forces on the cross section in lb per in. at the appropriate points,

then it is possible to show that these average radial stresses should each equal precisely the theoretical value of 0.1569 lb per in. per lb of load.

The proof of this statement follows from a consideration of the static equilibrium of a free-body diagram of a portion of the shell. This free-body is the upper portion of that section of shell which would be cut by a plane parallel to the plane of the bounding circle. The load P acts normal to this cutting plane.

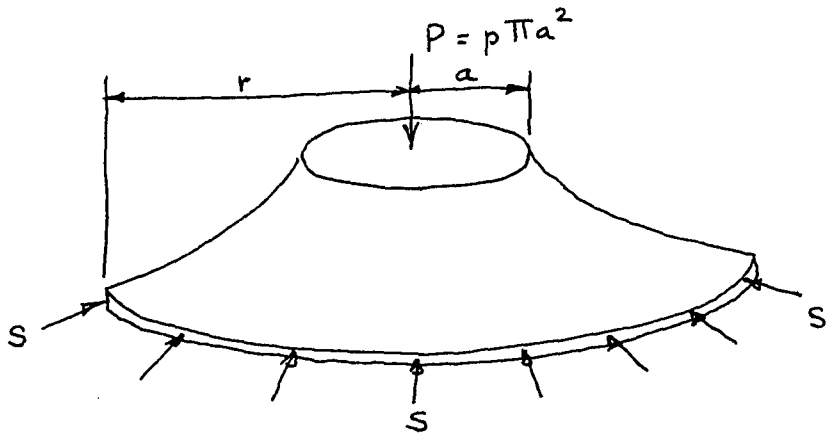

Because of symmetry, the normal stress S is assumed to be constant around the cut circle as shown. The slope at which the resultant stress S acts is assumed to be equal to the slope of the middle surface of the shell in the radial direction at that point. This slope may be represented by

$$\frac{dz}{dr} = -\left[\left(\frac{2rs}{pa^2}\right)^2 - 1\right]^{-1/2} = -\left[\left(\frac{2\pi rs}{P}\right)^2 - 1\right]^{-1/2}.$$

For the dimensions of the circular shell, this expression becomes $$\frac{dz}{dr} = -\left[(.9858\,r)^2 - 1\right]^{-1/2}.$$

The vertical component of S will then be

$$S\left[\frac{\left[(.9858\,r)^2-1\right]^{-1/2}}{\left[1+\frac{1}{(.9858\,r)^2-1}\right]^{1/2}}\right]$$ acting upward.

This reduces to $$S\left[\frac{1}{.9858\,r}\right].$$

Summing forces vertically than gives

$$P = 2\pi r S\left[\frac{1}{.9858\,r}\right]$$

and $$\frac{S}{P} = \frac{.9858}{2\pi} = 0.1569 \text{ lb per in. per lb.}$$

A few possible reasons for the differences between the observed and the theoretical values for S/P for the gage points in general are the following:

1. The shell may have possessed irregularities. This item may have various effects on the stress distribution. For example, an effective thickness at a gage point of 0.012 in. more than the observed thickness at the specific point would decrease

the observed S/P by approximately 10 per cent. This follows from the previously cited relationship for S/P in terms of observed strains, elastic constants, loads and thickness. Similarly, if the effective thickness were 0.012 in. less than the observed value, the observed value of S/P would be approximately 10 per cent greater. The same argument holds for errors in thickness measurements.

2. The properties of the material in the shell may have differed from those of the test cylinders. An increase of 10 per cent or approximately 7.9×10^4 psi in the modulus of elasticity would increase the observed values of S/P approximately 10 per cent, other items remaining constant. These figures also follow from the relationship which was previously used to convert values of unit strain per lb of load to values of S/P.
3. The testing apparatus may not have produced the proper load transfer. This might have a tendency to promote non-symmetrical stress distribution, bending, and the development of shearing stresses.
4. The SR-4 gages together with the nitro-cellulose cementing material may have altered the stiffness of the 0.120 in.-thick shell in the vicinity of the gages. R. C. Dove (3) considered this factor for materials of low stiffness and for various

thicknesses. In his paper he presents a nomograph which predicts the stiffening effect for A-1 type gages applied to both sides of a 3/8 in. strip of material of arbitrary thickness. For the specific case of the plaster-of-paris used in this investigation, the stiffening effect is approximately 1.065 if the material is assumed to be 0.120 in. thick. According to this consideration, the observed values should be multiplied by 1.065 to obtain actual values of S/P. The average S/P values for gage point 2 for the circular shell change from 0.138, 0.132, and 0.141 for the tangential, radial, and diagonal gages respectively to 0.147, 0.141, and 0.150. These values are closer to the theoretical of 0.157.

5. Shearing stresses which act in a direction normal to the central surface of the shell may have developed. These stresses were assumed to be equal to zero in the development of the characteristic equations. The existence of shears of this type would affect the magnitude of the predicted normal radial stress at a given cross-section for the type of shell tested.

6. Saint-Venant's principle may not have been fully realized, particularly in the case of the edge gage points. Timoshenko (16) on page 53 shows stress

distributions which occur at various distances along the axis of a two-dimensional plate which is subjected to concentrated axial loads. It is interesting to observe that at a distance equal to the width of the plate, the stress distribution is practically uniform, varying from 0.973 to 1.027. If it is assumed that a thin radial section of the shell approximates the plate, then at a distance of 0.120 in. from the edge, stress concentration may be largely eliminated. Certainly it would be expected that at a distance of 0.500 in., which was the minimum gage clearance at the edges, this type of edge effect would not be critical.

7. Droplets of soap solution may have collected on the aluminum disk while measurements of the membrane were being taken. An average drop of the solution weighed 0.042 gm. Since the weight of the aluminum disk was only 0.211 gm., the addition of one drop of solution would increase the effective weight of the disk approximately 20 per cent. This increase in weight would reduce the value of S_m/P_m by 20 per cent, since the surface tension S_m is considered a constant. Because of the linear relationship between S_m/P_m and S/P expressed as equation 16.1, there would be a corresponding decrease in the theoretical value of S/P of 20 per cent.

The average observed value for S/P for the tangential gage at point 2 is 0.138 in. lb per lb which compares favorably with the value of 0.132 in. lb per lb for the radial direction at the same point. This would indicate that constant membrane stress distribution was close to a reality at gage point 2 for the circular shell. It will be observed, however, that both of these values are below the value of 0.157, which was predicted by the theory. It is interesting to note that gages 2t and 2r were theoretically in the directions of principal stress at point 2. The average slope for the diagonal gage 2d should then be equal to $\frac{1}{2}$ the sum of the slopes for 2t and 2r. The average value of S/P for gage 2d was 0.141 and $\frac{1}{2}$ the sum of the slopes for 2t and 2r is 0.135. It is felt that these values are sufficiently close to one another to conclude that for all practical purposes, symmetry was attained and constant compressive membrane stress distribution occurred at point 2 of the circular shell; however, the value of this stress was apparently below that predicted by the theory. Possible reasons for this difference were previously stated.

At the outer edge for gage point 1 it will be observed that the average value of S/P was extremely low and in fact was in tension on the top surface. This measurement provides evidence to the fact that the theoretical boundary conditions of constant compressive stress S were not provided. The edge beam should probably have been back-loaded or prestressed

to compensate for the outward strains which were produced as the shell thrust against it. Proper prestressing would have provided a closer approximation to the theoretical boundary conditions and would have undoubtedly reduced the magnitude of the variation of normal stresses throughout the shell. This item should certainly not be overlooked if the method presented here is applied to actual structures.

At the edge, close to the load, the average tangential value of 0.103 was below the theoretical value of 0.157. In addition to the reasons given previously for possible variations, it should be noted that the center portion of the shell immediately under the rubber stopper was thickened to approximately $\frac{1}{2}$ in. to prevent local failure at the point of application of the concentrated load. This thickening might have tended to prevent the strains which would have normally occurred in the tangential direction at point 3. Any such effect would tend to reduce the value for S/P which was observed at this point.

The observed value for the slope of the load-deflection curve for the centerpoint was 48×10^{-6} in. per lb. The theoretical value from Fig. 16 was 48.8×10^{-6} in. per lb. The closeness of these values indicates that the average membrane stress was very close to the predicted value; however, compensating differences could certainly be present.

For the square shell, $E = 0.814 \times 10^{6}$ psi and $\mu = 0.229$. The thickness, t, varied from 0.104 in. to 0.127 in.

Observed values of S/P for this shell were determined from the slopes of the load-strain curves of Table 2 by the same method as was used for the circular one. These values are listed in Table 4.

Table 4. Comparison of values of S/P[a] for gage points on square shell

Point[b]	Observed S/P	Theoretical S/P	Point	Observed S/P	Theoretical S/P
1tt	-0.001	0.250	4tt	0.245	0.250
1tb	0.040	0.250	4tb	0.250	0.250
Avg.[c]	0.020	0.250	Avg.	0.248	0.250
1rt	0.056	0.250	4rt	0.328	0.250
1rb	0.397	0.250	4rb	0.188	0.250
Avg.	0.226	0.250	Avg.	0.258	0.250
2tt	0.214	0.250	5tt	0.111	0.250
2tb	0.181	0.250	5tb	0.103	0.250
Avg.	0.198	0.250	Avg.	0.107	0.250
2rt	0.418	0.250	5rt	0.144	0.250
2rb	0.076	0.250	5rb	0.137	0.250
Avg.	0.247	0.250	Avg.	0.140	0.250
2dt	0.368	0.250	5dt	0.104	0.250
2db	0.012	0.250	5db	0.142	0.250
Avg.	0.190	0.250	Avg.	0.123	0.250
3tt	0.248	0.250	6tt	-0.005	0.250
3tb	0.105	0.250	6tb	-0.028	0.250
Avg.	0.176	0.250	Avg.	-0.016	0.250
3rt	0.168	0.250	6rt	-0.024	0.250
3rb	0.181	0.250	6rb	0.123	0.250
Avg.	0.174	0.250	Avg.	0.054	0.250

[a]Values of S/P are in units of lb per in. per lb of load. Compressive values are positive; tensile values are negative.

[b]Notation is as described in Fig. 13.

[c]Average values represent membrane stresses.

Theoretical values for the quantity S/P and for the slope of the load-deflection curve for the centerpoint are developed in Fig. 17 by methods similar to those used on the circular shell.

FOR THE PREDICTION OF THE THEORETICAL VALUE OF S/P FOR THE SQUARE SHELL, CONSIDER THE FOLLOWING:

$$\frac{S}{P} = \frac{1}{n_1}\frac{S_m}{P_m} \quad \text{from eqn. 16.1}$$

$$= \frac{1}{2.5}(.6275) = 0.251.$$

FOR THE PREDICTION OF THE SLOPE OF THE LOAD-DEFLECTION CURVE FOR THE SQUARE SHELL:

$$V = \frac{\sigma^2(1-\mu)}{E}\iiint dx\,dy\,dz = \frac{\sigma^2(1-\mu)}{E}\times(\text{volume}) \quad \text{from 16.2.}$$

The volume may be approximated by considering the square shell to be a surface of revolution whose outer radius is such that it encloses an area which is equal in plan to that of the square shell. The inner radius is the same as that of the square shell. By the theorem of Pappus,

$$\text{Volume} = 2\pi\,\bar{r}\cdot(\text{area of generator})$$

$$= 2\pi(3.90)(0.74) = 18.15 \text{ in.}^3$$

$$V_{\text{for 1 lb load}} = 18.15(.251)^2\left(\frac{1-0.229}{(.115)^2(.814\times10^6)}\right) \text{ using 16.3}$$

$$= 81.8\times10^{-6} \text{ in.-lb/lb}.$$

$$m = 2(81.8\times10^{-6}) = 163.6\times10^{-6} \text{ in./lb} \quad \text{from 16.4}$$

$$m_{\text{observed}} = 136\times10^{-6} \text{ in./lb}.$$

Note that for the square shell $t=0.115$ in., $\mu=0.229$, $E=0.814\times10^6$ psi.

Fig. 17. Theoretical values for square shell

The theoretical value of $S_m/P_m = 0.6275$ was used here as in the first problem. This was possible because the same load was used to deflect each membrane. It was assumed that the surface tension of the soap film was the same in both cases. From Fig. 17 the resulting theoretical value for S/P is 0.250 lb per in. per lb.

It may be noted in Table 4 that many of the observed values of S/P do not agree in magnitude with the theoretical value although in all cases but one the average values are of the same sign as the theoretical. The possible reasons for disagreement stated previously for the circular shell apply equally as well here. The most pronounced disagreement occurs in gages 1 and 6, which are at the outer edges. Similar behavior was observed in the circular shell. Proper satisfaction of boundary conditions very probably would have improved this situation.

Gage points 2 and 5, which were not close to the edges, exhibit reasonably constant stress characteristics as far as the averages are concerned; however, it will be observed that these values are less than theoretical. The averages for gage point 4 are very close to the theoretical value. Those for point 3 are not as close but are within 0.002 lb per in. per lb of being constant. The behavior of these gages is better than that of gage 3 for the circular shell, which was in a similar position. This may have been due to the fact that gage points 3 and 4 for the square shell

were farther from the load point than was gage 3 on the circular shell, and therefore the boundary stresses existing at the center may not have had as great an effect at these points.

The observed slope of the load-deflection curve for deflection of the centerpoint of the square shell was 136×10^{-6} in. per lb. The theoretical value from Fig. 17 is 164×10^{-6} in. per lb based on the theoretical value for S/P of 0.250. The value for S/P which would yield 136×10^{-6} in. per lb as the predicted slope is 0.229 lb per in. per lb. This value is not out of line with those contained in Table 1. An increase in load on the original membrane of 4.09×10^{-5} lb, or 0.019 gm., would produce this change in the theoretical value of S/P. This increase in load could easily be attributed to the tendency for the soap solution to collect on the aluminum disk, since one drop of the solution weighs 0.042 gm.

Conclusions to the previous comparisons are given in the following section.

SUMMARY AND CONCLUSIONS

General characteristic differential equations which describe the surface that a shell structure must adopt in order that it resist prescribed normal pressure loads under constant membrane stress were developed. A membrane analogy was introduced which would give solutions to these differential equations for various problems. This analogy was considered particularly desirable for cases where closed-form mathematical solutions were difficult to obtain.

Methods of solution of the characteristic equations were illustrated on two examples. These examples involved shells circular and square in plan. The methods of solution used were integration of the differential equations, the inverse solution method and the solution by membrane analogy.

Plaster-of-paris shell structures were built to the dimensions predicted by the inverse solution and by the analogy which were the solutions to the non-linear characteristic equations for the two examples.

Tests were performed on the plaster shells, and strains and deflections were observed under action of the design load. Results of the tests were compared with theoretical values based on the application of principles of similitude and strain energy.

The following conclusions have been derived from this investigation:

1. Solutions to the characteristic differential equations give rise to shell structures which exhibit constant membrane stress characteristics at points removed from the boundaries when these shells are subjected to their design load.
2. It is necessary to provide proper boundary forces if constant membrane stress characteristics are desired throughout the shell.
3. Precision is essential if uniformity of stress and proper magnitudes of stress and deflections are important criteria.
4. Shells made of materials which are weak in tension will resist loads efficiently without reinforcement when they are designed by the proposed method. This conclusion may be reached by considering the 0.120 in.-thick plaster-of-paris shell shown in Fig. 18. This un-reinforced shell resisted a centered concentrated load of 685 lb before failing.

Fig. 18. Circular shell before and after failure load of 685 lb

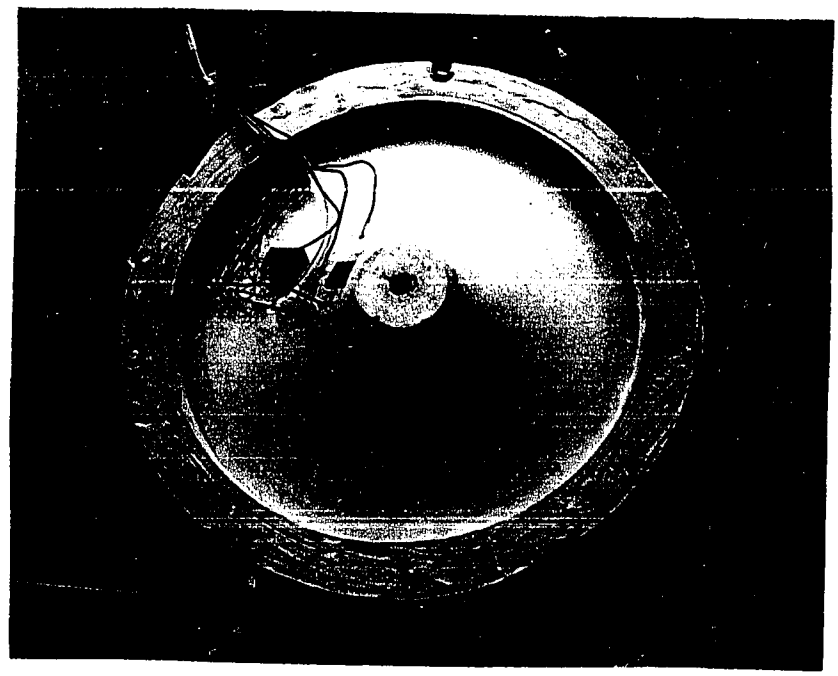

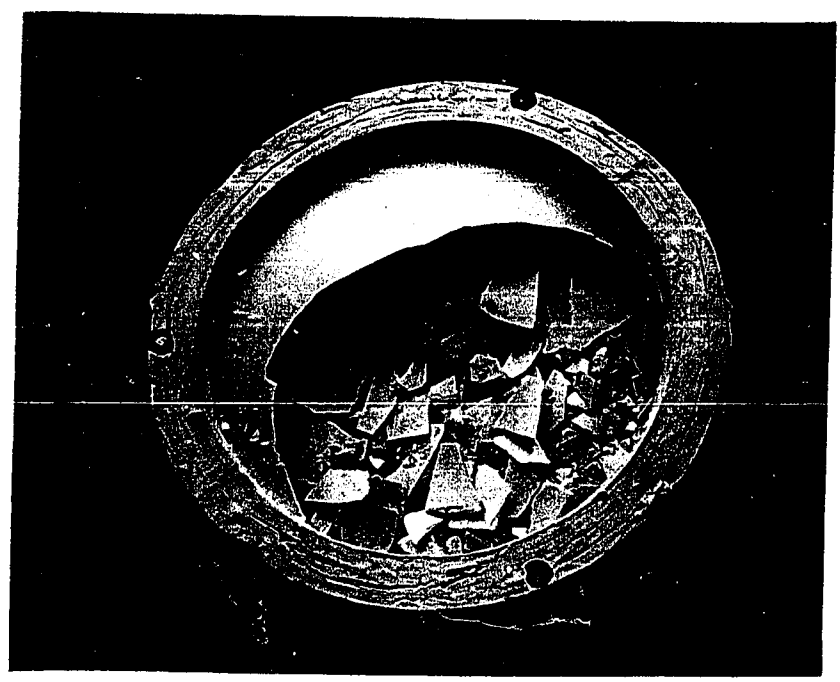

SUGGESTIONS FOR FURTHER STUDY

During the course of this investigation, many questions have arisen which might well be answered by further study of both an experimental and a theoretical nature. A few such studies are:

1. The existence of bending and shear stresses for shells satisfying the equations developed in this investigation should be studied in order that their magnitudes may be properly predicted.
2. Larger, more precise structures should be built and tested in order to better observe edge effects and in order to provide better comparisons with theoretical values of structural behavior.
3. The possibilities of using this method to design shell structures which may be prestressed by virtue of their action under external loads instead of by their action under prestressing cables lying in the shells should be investigated.
4. Further investigations should be conducted along the lines of the solution of the characteristic equations by analogies. One such analogy might be similar to that conducted by Friedmann et al. (4) which is the electrical conducting sheet analogy for the solution of the Poisson equation. The characteristic equation for the conducting sheet is basically

a Laplace equation but if the proper boundary voltages are supplied, Poisson equations may be solved. Characteristic equations 1.10 and 1.11 of this investigation were Poisson and Laplace equations respectively, therefore these equations could be solved by such an analogy.

5. The Laplaciometer described by Murphy and Atanasoff (10) and its application to the solution of the characteristic equations 1.10 and 1.11 should be investigated.
6. Effects of variation in thickness upon the resulting stresses in these shells should be examined.
7. The added precision offered by measuring the membrane by photogrammetric methods (1) should be investigated.
8. The solution of the appropriate differential equations by numerical methods such as finite differences should be investigated. For efficiency, these solutions should probably make use of digital computers.

LITERATURE CITED

1. Bonanno, F. R. Torsion constants of certain cross-section by non-topographic photogrammetry. Photogrammetric Engineering 25: 803-809. 1958.

2. Borkhausen, Von G. Neure formen für flüssigkeitsbehälter. Zeitschrift des vereines deutscher Ingenieure 44: 1594-1599; 1681-1685. 1900.

3. Dove, R. C. Strain measurement errors in materials of low modulus. American Society of Civil Engineers, Proceedings. 81, No. 691. 1955.

4. Friedmann, N. E., Yamamoto, Y. and Rosenthal, D. Solution of torsional problems with the aid of the electrical conducting sheet analogy. Proceedings of the Society for Experimental Stress Analysis 13, No. 2: 1-6. 1956.

5. Horne, M. R. Shells with zero bending stresses. Journal of the Mechanics and Physics of solids 2: 117-126. 1954.

6. Jenkins, R. J. Theory of new forms of shell. Proceedings of a symposium on concrete shell roof construction, July 2-4, 1952. pp. 127-148. Cement and Concrete Association. London. 1954.

7. Karas, Von K. Die Auswölbungen der Kreis- und Kreisringmembranen unter hydrostatischem Druck. Ingenieur-Archiv. 25: 359-380. 1957.

8. Merrifield, C. W. Determination of the form of the dome of uniform stress. London Mathematical Society Proceedings. 5: 113-119. 1874.

9. Murphy, G. Similitude in engineering. 1st ed. Ronald. New York, N. Y. 1950.

10. _____ and Atanasoff, J. V. A mechanical device for the solution of equations involving the Laplacian operator. Iowa Engineering Experiment Station Bulletin 166. Iowa State College. 1949

11. Nash, W. A. Bibliography on shells and shell-like structures. U. S. Navy Department. David W. Taylor Model Basin. TMB (Taylor Model Basin) Report 863. 1954.

12. Plateau, J. The figures of equilibrium of a liquid mass. Annual Report of the Board of Regents of the Smithsonian Institution, 1863: 207-285. Gov't. Printing Office. Washington, D. C. 1872.

13. _____ The figures of equilibrium of a liquid mass. Annual Report of the Board of Regents of the Smithsonian Institution, 1864: 285-369. Gov't. Printing Office. Washington, D. C. 1872.

14. _____ The figures of equilibrium of a liquid mass. Annual Report of the Board of Regents of the Smithsonian Institution, 1865: 411-435. Gov't. Printing Office. Washington, D. C. 1872.

15. Poschl, T. Kuppeln mit gleichen Normalspannungen. Der Bauingenieur. 8: 624-628. 1927.

16. Timoshenko, S. and Goodier, J. N. Theory of elasticity. 2nd ed. McGraw-Hill Book Co., Inc. New York, N. Y. 1951.

17. Wang, C. T. Applied elasticity. McGraw-Hill Book Co., Inc. New York, N. Y. 1953.

ACKNOWLEDGMENTS

The author would like to acknowledge persons and organizations for their help in this investigation.

To the members of his graduate committee, who have given invaluable assistance and advice in the completion of this project, he extends his appreciation. Particular thanks is given the chairman of his committee, Dr. Glenn Murphy, who spent considerable time counselling, reviewing, and offering suggestions on the different aspects of the investigation.

The author is indebted to the National Science Foundation which awarded him a twelve-month Science Faculty Fellowship to facilitate his research and enable him to spend full time in the pursuit of his studies.

To Dr. George Town and the Iowa Engineering Experiment Station, thanks is due for invaluable encouragement and assistance.

Without the help of these individuals and organizations, this investigation may not have become a reality.